Aus der Klinik und Poliklinik für Unfall-, Hand-, Plastische und
Wiederherstellungschirurgie
der Universität Würzburg

Direktor: Professor Dr. med. Rainer H. Meffert

Resveratrol Counteracts IL-1β-mediated Impairment of Extracellular Matrix Deposition in 3D Articular Chondrocyte Constructs

-

Resveratrol wirkt der IL-1β-vermittelten Beeinträchtigung von Extrazellulärmatrix-Deposition in 3D Konstrukten aus artikulären Chondrozyten entgegen

Inauguraldissertation

zur Erlangung der Doktorwürde der
Medizinischen Fakultät
der
Julius-Maximilians-Universität Würzburg

vorgelegt von
Sebastian Frischholz
aus Bonn

Würzburg, Dezember 2020

Referent: **Prof. Dr. rer. nat. Torsten Blunk**
Klinik und Poliklinik für Unfall-, Hand-, Plastische und Wiederherstellungschirurgie der Universität Würzburg

Koreferent: **Prof. Dr. rer. nat. Uwe Gbureck**
Lehrstuhl für Funktionswerkstoffe der Medizin und der Zahnheilkunde der Universität Würzburg

Dekan: **Prof. Dr. med. Matthias Frosch**

Tag der mündlichen Prüfung: 17. März 2021

Der Promovend ist Arzt.

Contents

Statement on Copyright and Self-plagiarism

The data presented in this thesis have been partially published in the *Journal of Tissue Engineering and Regenerative Medicine* as an original article entitled "Resveratrol counteracts IL-1β-mediated impairment of extracellular matrix deposition in 3D articular chondrocyte constructs". In accordance with the regulations of the parent publisher Wiley (License CC BY-NC 4.0), data, text passages and illustrations from the final published manuscript were used in identical or modified form in this thesis. The Figures 3.1, 4.2, 4.3, 4.5, and 4.6 within this thesis have been previously published in a modified or identical design in the original article:

Frischholz, S., Berberich, O., Böck, T., Meffert, R., & Blunk, T. (2020). Resveratrol counteracts IL-1β-mediated impairment of extracellular matrix deposition in 3D articular chondrocyte constructs. Journal of Tissue Engineering and Regenerative Medicine, 14, 897-908. doi: 10.1002/term.3031

Statement of individual contributions: I, Sebastian Frischholz, designed the study, conducted the experiments, evaluated the data and wrote the manuscript. Oliver Berberich contributed to the study design, methods refinement, and was involved in the proofreading. Thomas Böck supported the methods refinement and data collection. Rainer Meffert was involved in the study design and proofreading. Torsten Blunk, as principal investigator, participated in the study design, data interpretation, manuscript writing, and proofreading.

Part I

Introduction

Chapter 1

Introduction

1.1 Articular cartilage: structure and function

As exceptional connective tissue articular cartilage is coating the surface area of articulating bones in all diarthrodial joints (Armiento *et al.*, 2018; Mow *et al.*, 2002). Thereby, it allows both low-friction articulation and distribution of loads to the subchondral bone (Carballo *et al.*, 2017; Pan *et al.*, 2009). Still, as mature articular cartilage is an avascular, aneural, and alymphatic tissue (Krishnan & Grodzinsky, 2018), its ability to self-repair is very limited.

The chondrocyte as sole cell type within cartilage tissue is highly specialized in maintaining a unique extracellular matrix (ECM) composition while only occupying about 5 % of the tissue's wet weight (Ulrich-Vinther *et al.*, 2003).

Cells surrounded by a pericellular matrix are organized in microanatomical units referred to as chondrons (Poole, 1997). Biochemically, the solid matrix of mature articular cartilage contains mainly fibrillar collagen and negatively charged proteoglycans (Mow *et al.*, 2002). The polyanionic proteoglycans attract interstitial ions and water osmotically thus providing compressive resilience to the tissue (Carballo *et al.*, 2017; Kempson *et al.*, 1970; Linn *et al.*, 1965; Maroudas *et al.*, 1991). Proteoglycans consist of a core protein chain covalently bound to sulphated glycosaminoglycan (GAG) side chains, which in turn are carbohydrates constituted of repeating disaccharide units. Among others, aggrecan is the prevailing proteoglycan in articular cartilage forming large complexes with hyaluronic acid (hyaluronan) (Culav *et al.*, 1999).

Complementary to proteoglycans, the collagen fibril network is capable of resisting tensile stress. Decisive biomechanical properties are exhibited by assembly and cross-linking of triple helices, which themselves consist of three polypeptide chains (Mouw *et al.*, 2014). In total, the collagen framework constitutes about two thirds of the dry weight of articular cartilage (Eyre, 2004). Whereas collagen type II is predominant (> 90 %), others like collagen type IX and type XI are relevant for cross-linking interactions (Eyre, 2004). Apart from that, expression of different types of collagen within articular cartilage is associated with pathological conditions. Such is revealed for collagen type I in fibrocartilage and collagen type X in hypertrophic chondrocytes (Armiento *et al.*, 2019). Anatomically and biochemically hyaline, articular cartilage is composed of consecutive zones with unique ECM architecture (Figure 1.1).

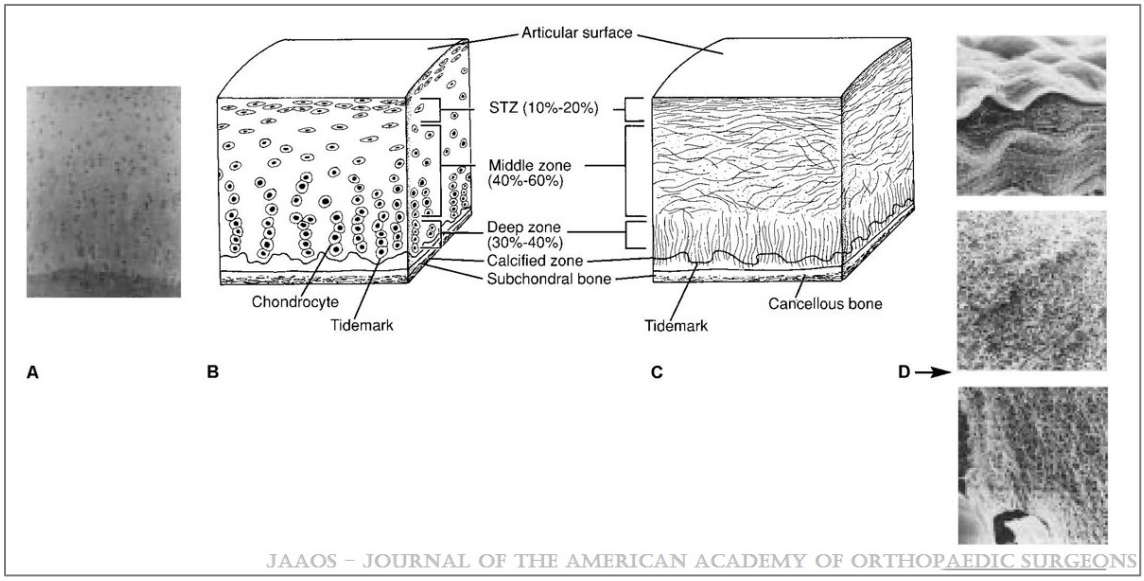

Figure 1.1. Structure of articular cartilage. "(**A**) Histologic section of cartilage from a young, healthy adult shows even safranin O staining and distribution of chondrocytes. (**B**) Schematic diagram of chondrocyte organization in the three main zones of the uncalcified cartilage (STZ = superficial tangential zone), the tidemark, and the subchondral bone. (**C**) Sagittal cross-sectional diagram of collagen fiber architecture shows the three salient zones of articular cartilage. (**D**) Scanning electron micrographs depict arrangement of collagen in the three zones (top = STZ; center = middle zone; bottom = deep zone)."
Reproduced with permission from Wolters Kluwer Health, Inc.: Buckwalter, J. A. *et al.* (1994) Restoration of Injured or Degenerated Articular Cartilage. *Journal of the American Academy of Orthopaedic Surgeons.* doi:10.5435/00124635-199407000-00002).

With depth from the surface, the concentrations of fibrillar collagen and proteoglycans both shift (Aydelotte *et al.*, 1988; Malda *et al.*, 2012). Besides, morphology, density, and organization of chondrocytes differ across the depth of articular cartilage (Armiento *et al.*, 2018). The superficial zone is characterized by elongated cells in high density with tangentially orientated collagen fibers and lower amount of proteoglycan than in deeper layers (Johnstone *et al.*, 2013; Poole *et al.*, 1983) (Figure 1.1). Thus, it can withstand shear force at the surface area. In the middle zone, spherical chondrocytes are placed in a more randomly organized collagen network due to curved configuration of fibers (Carballo *et al.*, 2017). The deep zone is marked by large cells located in columns, perpendicular collagen fibers, and the highest proteoglycan content (Aydelotte *et al.*, 1988; Johnstone *et al.*, 2013). A further calcified zone forms conjunction to the subchondral bone (Figure 1.1). Synovial fluid (SF) within the joint contains hyaluronic acid, which exhibits high viscosity, lubricin (proteoglycan 4), and phospholipids (Schmidt *et al.*, 2007). Therefore, besides containing nutrients, SF achieves boundary lubrication and enables joint movement with a very low friction coefficient (Armiento *et al.*, 2018).

As mature articular cartilage is an avascular, aneural, and alymphatic tissue with a very limited ability to self-repair (Krishnan & Grodzinsky, 2018), there are constant efforts to advance repair and tissue engineering techniques.

1.2 Repair and tissue engineering techniques for articular cartilage

Chondral defects following traumatic injury continue to be a tremendous challenge in orthopedics and traumatology, increasing the risk of developing

secondary osteoarthritis (OA) four-fold (Muthuri *et al.*, 2011). Whereas partial-thickness defects do not permeate into the subchondral bone and thus do not show spontaneous repair, full-thickness defects penetrate the subchondral bone exhibiting limited repair potential by local inflow of blood and mesenchymal stem cells (MSCs) (Carballo *et al.*, 2017). Over the last decades, different approaches for articular cartilage repair have emerged and progressively been tested clinically. Whereas some techniques are currently applied regularly, others are still in development. Still, regenerative techniques could postpone or prevent the need for total joint replacement (Armiento *et al.*, 2018). Makris *et al.* seized the idea of a tissue engineering paradigm including three major strategies: scaffold-based implants without cells, cell-seeded scaffolds emulating native articular cartilage, and scaffold-free, cell-based biomimetic techniques (Makris *et al.*, 2015) (Figure 1.2).

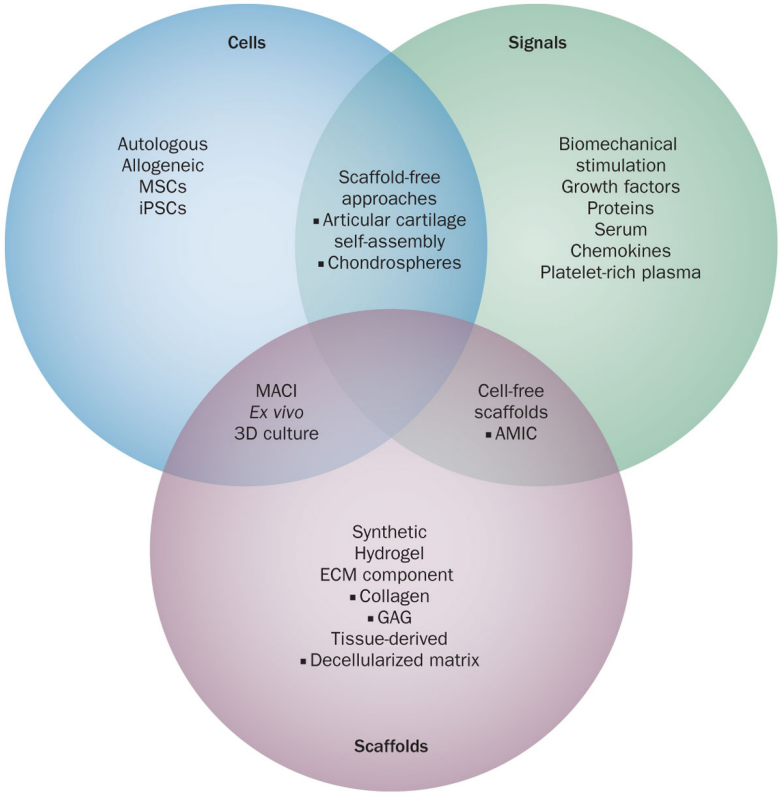

Figure 1.2. Articular cartilage tissue engineering strategies. Reproduced with permission from Springer Nature: Makris, E. A. *et al.* (2015) Repair and tissue engineering techniques for articular cartilage. *Nature Reviews Rheumatology*. doi: 10.1038/nrrheum.2014.157.

Prevailing repair and tissue engineering techniques for articular cartilage include microfracture, autologous chondrocyte implantation (ACI), as well as scaffold-based techniques (Makris *et al.*, 2015).

In microfracture, the subchondral bone is penetrated to improve infiltration of MSCs to the defect site (Makris *et al.*, 2015). Adversely, this technique often leads to the development of mechanically inferior fibrocartilage, which usually decays 18-24 months postsurgical (Kreuz *et al.*, 2006). Still, this simple, inexpensive technique exhibits a quick recovery time (Armiento *et al.*, 2018).

For ACI, autologous chondrocytes are harvested from a low-weight-bearing area of the joint and passaged *in vitro* (Makris *et al.*, 2015). Secondly, these cells are implanted into the defect region coated by a protecting membrane (Makris *et al.*, 2015). Case series with over 10 years follow-up have revealed positive clinical outcomes (Peterson *et al.*, 2010). Yet, this method is both time-consuming and costly, as two operations and an *in vitro* expansion are necessary. Further, a long recovery time of up to one year is crucial (Peterson *et al.*, 2000). A general drawback of using isolated and expanded cells is that subculture in monolayer causes phenotypic dedifferentiation towards a fibroblast-like morphology (Armiento *et al.*, 2018).

Scaffold-based techniques utilize 3D matrixes to increase control of the implant size and enhance a chondral phenotype. In matrix-induced autologous chondrocyte implantation (MACI) *in vitro* expanded chondrocytes are seeded on an absorbable porcine-derived collagen (type I and III) membrane for 3 days prior to implantation (Marlovits *et al.*, 2012; Makris *et al.*, 2015). Also, hyaluronic-acid-based scaffolds generated hyaline like cartilage after implantation in case series (Kon *et al.*, 2011; Marcacci *et al.*, 2005). Aside from that, an autologous

cartilage tissue implant consisting of a bovine type-I collagen matrix scaffold seeded with autogenous chondrocytes was shown to have enhanced clinical outcome compared to microfracture in a prospective, randomized clinical trial (Crawford *et al.*, 2012). Another option are novel cell-free biomaterials. In autologous matrix-induced chondrogenesis (AMIC), a matrix consisting out of collagen type I and type III is transplanted to the defect site enhancing early mechanical stability (Kusano *et al.*, 2012; Steinwachs *et al.*, 2019).

As further potential strategy scaffold-free approaches aim at exogenous stimulation of self-assembled neocartilage ex vivo prior to implantation into the defect site (DuRaine *et al.*, 2015; Makris, MacBarb *et al.*, 2013). Thereby, the chondrocyte phenotype can be promoted by various approaches. Aside from hypoxia (Thoms *et al.*, 2013), dynamic compression (Anderson & Johnstone, 2017) and growth factors such as transforming growth factor β1 (TGF-β1) or bone morphogenetic proteins (BMPs) (Kwon *et al.*, 2016) stimulate chondrogenic potential. Also, high cell-seeding density in pellet culture promotes the chondrocyte phenotype (Carballo *et al.*, 2017; Watt, 1988).
Indeed, small spheroids of neocartilage consisting of expanded autologous chondrocytes (Chondrospheres®) exhibit good integration within the defect. As completely biological and highly responsive tissue scaffold-free neocartilage is able to grow in size and fill the defect site (Huang *et al.*, 2016).
Also, application of juvenile allogeneic chondrocytes seems promising as they exhibit greater chondrogenic potential than adult cells (Adkisson *et al.*, 2010).

Whereas these repair and tissue engineering techniques are already applied for chondral defects following traumatic injury or malalignment, systemic person-level factors contributing to cartilage deterioration are scarcely addressed.

1.3 Osteoarthritis

1.3.1 Epidemiology and definition

As severe joint affecting disease (OA) is an increasing challenge not only regarding the afflicted person's joint function and life quality (Robinson *et al.*, 2016), but also to public health. According to estimates, prevalence of OA as the most common form of arthritis is at least 19 % in U.S. adults ≥ 45 years, and over the next decades increasing numbers must be assumed (Lawrence *et al.*, 2008; Wallace *et al.*, 2017). Despite of that, estimated rates show wide variations as they are influenced by case definition (radiographic, clinical, or pathological OA), the evaluated cohort (i.e. developed versus developing countries), and investigated joints (Palazzo *et al.*, 2016).

Overall, the 2010 WHO Global Burden of Disease Study ranked OA as 11th cause of years lived with disability worldwide. Thereby, OA of the knee accounted for 83 % of the total OA burden (Vos *et al.*, 2012).

Radiographic OA is commonly assessed using the Kellgren and Lawrence score, which includes the formation of osteophytes, narrowing of joint space, sclerosis of subchondral bone, small pseudocystic areas, and altered shape of the bone ends (Kellgren *et al.*, 1957; Petersson *et al.*, 1997). In contrast, criteria of the American College of Rheumatology have been proposed for definition of clinical OA. These include pain, erythrocyte sedimentation rate (ESR), and morning stiffness (Altmann *et al.*, 1991).

1.3.2 Pathogenesis

Various studies focused on revealing the pathogenesis of OA in order to find therapeutic approaches (Leung *et al.*, 2014; Sokolove *et al.*, 2013; Xia *et al.*, 2014). As progressive multifactorial disease, OA is eventually disturbing the functional integrity of synovial joints (Mobasheri *et al.*, 2017). Risk factors can be differentiated into person-level factors (age, gender, obesity, and genetics) and joint-level factors (traumatic injury, excessive loading, and malalignment) (Palazzo *et al.*, 2016), and are partly interdependent (Figure 1.2).

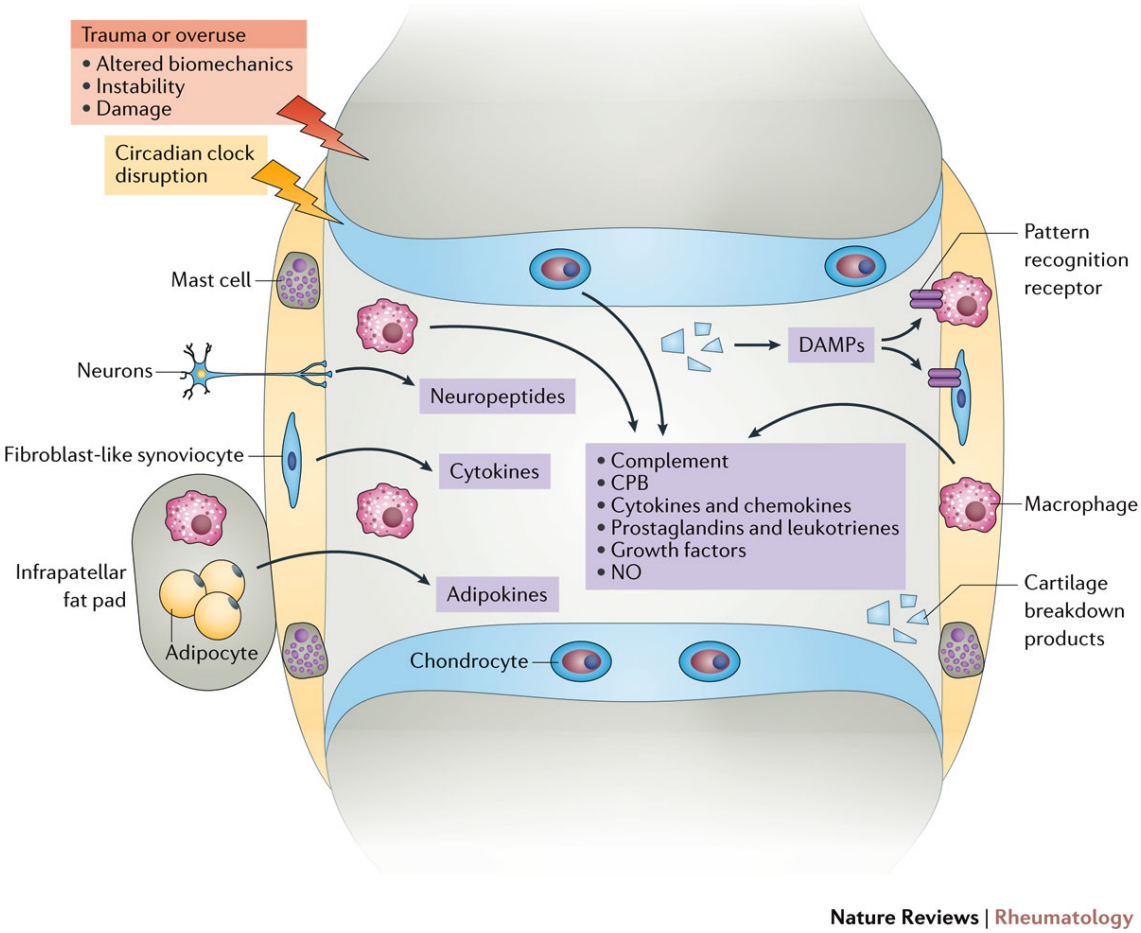

Figure 1.3. Pathogenesis of osteoarthritis. Reproduced with permission from Springer Nature: Robinson, W. H. *et al.* (2016) Low-grade inflammation as a key mediator of the pathogenesis of osteoarthritis. *Nature Reviews Rheumatology*. doi:10.1038/nrrheum.2016.136.

1.3.3 Person-level risk factors

Increasing age represents the most prominent risk factor for OA (Johnson & Hunter, 2014). In this context, cellular senescence accompanied with an altered secretory profile and elevated levels of reactive oxygen species (ROS) contribute to OA (Loeser *et al.*, 2016). Chondrocytes from patients with OA exhibited decreased mitochondrial mass and mitochondrial DNA (Wang *et al.*, 2015) and normal chondrocytes, upon mitochondrial dysfunction, showed an increased responsiveness to inflammatory cytokines (Vaamonde-García *et al.*, 2012). Moreover, studies have shown disturbances in various signaling pathways: besides a decrease of insulin-like growth factor 1 (IGF-1) signaling (Yin *et al.*, 2009), activation of catabolic mitogen-activated protein kinase (MAPK) signaling pathways was increased (Loeser *et al.*, 2014).

Changes in the ECM involve a marked increase in the formation of advanced glycation end-products (AGEs) (Lotz & Loeser, 2012). This alteration results in enhanced cross-linking of collagen molecules and thus adverse biomechanical properties such as increased stiffness (Lotz & Loeser, 2012). Moreover, deposition of crystals containing calcium represents a hallmark of aging in articular cartilage (Mitsuyama *et al.*, 2007).

Apart, the presence of sex differences in the prevalence of OA has been demonstrated. In particular, women are at higher risk for developing knee and hand OA and tend to have more severe knee OA (Srikanth *et al.*, 2005).

In terms of genetics, estimated heritability is 60 % for hand and hip OA and 40 % for knee OA shown by classic twin studies (Spector & MacGregor, 2004), with various gene loci under consideration (Johnson & Hunter, 2014).

Furthermore, obesity has been identified as dose-dependent risk factor for knee OA: with every five-unit increase in body mass index (BMI), an associated 35 % increase in risk for knee OA was found (Jiang *et al.*, 2012). Interestingly, besides mediating detrimental biomechanical effects, obesity is associated with hand OA (Grotle *et al.*, 2008). Thus, alterations of systemic metabolism seem to play a substantial role in the pathogenesis of OA. Indeed, metabolic changes linked to obesity, physical inactivity, insulin resistance, and type 2 diabetes mellitus promote inflammatory pathways (Mobasheri *et al.*, 2017). Especially adipokines enhance progression of OA by inducing pro-inflammatory cytokines and degenerative enzymes, resulting in a chronic low-grade inflammatory status (Wang *et al.*, 2015). Moreover, a metabolic switch to anaerobic glycolysis aggravates an acidic milieu and adenosine triphosphate (ATP) depletion (Lane *et al.*, 2015; Maneiro *et al.*, 2003). Notably, loss of weight in obese patients with knee OA improved pain and joint function, while decreasing low-grade inflammation (Richette *et al.*, 2011).

1.3.4 Joint-level risk factors

In terms of joint-level factors, age-related sarcopenia combined with an increase in fat mass may alter joint loading and decrease dynamic joint stability (Litwic *et al.*, 2013). In young adults OA is most often caused by traumatic injury. The isolated rupture of the anterior cruciate ligament (ACL) results in a 13 % prevalence of post-traumatic knee OA after 10 to 15 years (Øiestad *et al.*, 2009). However, ACL rupture is often combined with additional damage to articular cartilage, subchondral bone, collateral ligaments, and especially menisci. Importantly, meniscal damage occurs in approximately 65 % of ACL injuries

(Slauterbeck *et al.*, 2009) and is related to a higher prevalence of knee OA, ranging between 21 % and 48 % (Øiestad *et al.*, 2009).

Also, excessive loading such as highly repetitive and high-impact physical stress in elite-level athletes appears to increase risk for radiographic hip and knee OA (Johnson & Hunter, 2014). Furthermore, hip OA has been linked to persistent standing and lifting (Croft *et al.*, 1992).

Regarding knee OA progression, there is a strong association between malalignment of the joint and enhanced structural deterioration (Sharma *et al.*, 2001). Whereas varus alignment was accompanied by a four-fold increase in risk for medial progression of knee OA, valgus alignment increased risk for lateral progression two-fold (Cerejo *et al.*, 2002).

1.3.5 Inflammation

Interdependent with the above-mentioned risk factors, low-grade inflammation plays a pivotal role in the multifactorial pathogenesis of OA (Blagojevic *et al.*, 2010; Felson *et al.*, 2000; Lopes *et al.*, 2017; Robinson *et al.*, 2016). In terms of that, OA does not only compromise articular cartilage itself but also other areas of the joint including condensation of the subchondral bone, development of osteophytes, joint capsule hypertrophy, plus, especially, synovitis (Loeser *et al.*, 2012). By resulting in high levels of plasma proteins, complement components, and cytokines in the synovial fluid, this synovial inflammation affects articular cartilage likewise (Gobezie *et al.*, 2007; Pelletier *et al.*, 2001; Sokolove *et al.*, 2013). Eventually, this process is associated with enhanced cartilage loss,

reduced mobility, and increased radiographic grades (Guermazi *et al.*, 2011; Robinson *et al.*, 2016).

Besides various other inflammatory mediators like growth factors, chemokines, adipokines and prostaglandins being present in OA joint tissues and fluids, inflammatory cytokines such as interleukin 1β (IL-1β) and tumor necrosis factor α (TNFα) and have been related to cartilage catabolism and extracellular matrix breakdown in particular (Lopes *et al.*, 2017; Sokolove *et al.*, 2013; Goldring *et al.*, 1994; Endres *et al.*, 2010; Martel-Pelletier *et al.*, 2003). Especially IL-1β is subject of current research and has been shown to exhibit potent catabolic effects on cartilage tissue (Jenei-Lanzl *et al.*, 2019). At the molecular level, detrimental effects were in part exerted via activation of nuclear factor κB (NF-κB), mitogen-activated protein kinase (MAPK), and activator protein 1 (AP-1) signaling (Chowdhury *et al.*, 2008). Also, innate immune mechanisms such as recognition of damage-associated molecular patterns (DAMPs) and initiation of the complement system can activate macrophages (Foell *et al.*, 2007), consequently producing inflammatory mediators such as IL-1β and TNFα.

Chondrocytes cause degradation of ECM constituents via proteinases such as matrix metalloproteinases (MMPs) (Carballo *et al.*, 2017). MMP13 exhibits the highest expression of any proteinase in OA and can degrade both collagen type II and aggrecan (Little *et al.*, 2009; Rengel *et al.*, 2007).

1.3.6 Therapy

Although systemically applied anti-IL-1β or anti-TNF treatments are licensed for therapy of rheumatoid arthritis (RA), they have shown no satisfying benefit in OA clinical studies (Cohen *et al.*, 2011; Verbruggen *et al.*, 2012). This might

partly be due to the circumstance that inflammation in OA, as compared to RA, is more chronic, relatively low-grade and caused mainly by the innate immune system (Robinson *et al.*, 2016). Still, current treatments such as common nonsteroidal anti-inflammatory drugs (NSAIDs) and joint replacement primarily address end-stage symptoms (Tonge *et al.*, 2014; Mobasheri, 2013). A promising approach are the aforenamed cell-based therapies. Yet, despite vast improvements in repair and tissue engineering techniques for articular cartilage defects, serious challenges remain confining broader clinical applicability. Besides phenotypic instability of the repair tissue and poor integration with adjacent native tissue, pro-inflammatory cytokines exhibit potent catabolic effects on cartilage tissue (Kwon *et al.*, 2016) (Figure 1.4). Thus, a combination of cell-based therapy and anti-inflammatory agents appears desirable to effectively treat OA joints.

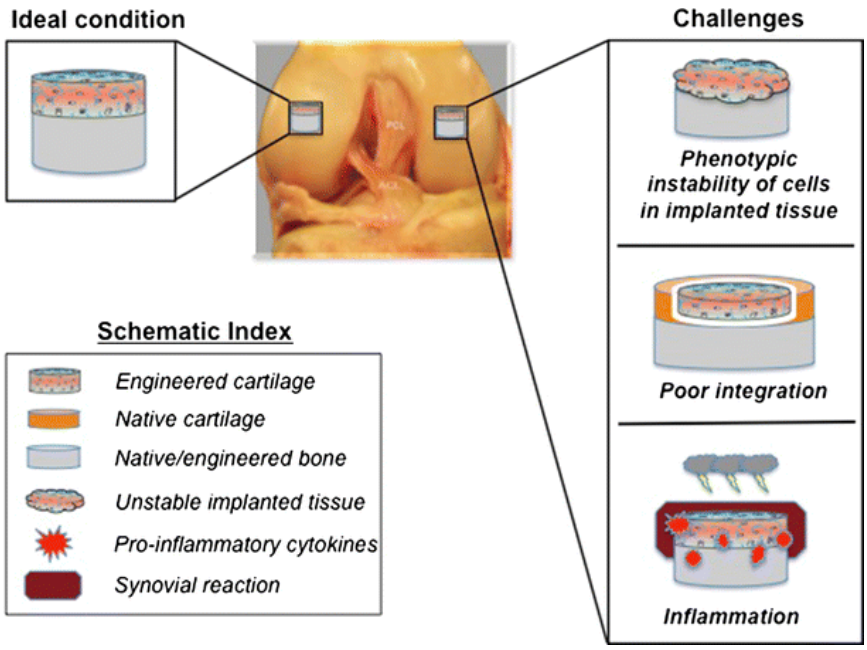

Figure 1.4. Challenges in articular cartilage repair and tissue engineering techniques. Reproduced with permission from Springer Nature: Kwon, H. *et al.* (2016) Articular cartilage tissue engineering: the role of signaling molecules. *Cellular and Molecular Life Sciences*. doi: 10.1007/s00018-015-2115-8.

1.4 Resveratrol: a potent anti-inflammatory drug for OA patients?

Resveratrol (RSV), a polyphenolic phytoalexin, might exhibit effective anti-inflammatory properties regarding inflammation in OA (Shen *et al.*, 2012; Deng *et al.*, 2019). As natural compound RSV can be found in the skin of red grapes, berries, and peanuts (Shen *et al.*, 2012).

Previous short-term studies revealed RSV-mediated signaling pathways and discovered that RSV is able to counteract IL-1β-mediated apoptosis of human articular chondrocytes *in vitro* (Csaki *et al.*, 2008; Csaki *et al.*, 2009; Dave *et al.*, 2008; Shakibaei *et al.*, 2008; Shakibaei *et al.*, 2011). Furthermore, in a short-term 48-hours experiment RSV was shown to inhibit IL-1β-induced down-regulation of collagen type II and aggrecan expression in MSC-derived chondrocytes (Lei *et al.*, 2008). Without regarding inflammatory conditions, Maepa *et al.* conducted a short-term study using monolayers of porcine articular chondrocytes cultured for four days. Within these experiments, RSV stimulated the expression of collagen type II at the mRNA and protein levels (Maepa *et al.*, 2016).

Besides mentioned studies, which primarily considered short-term effects and were conducted mostly in monolayer cultures, a hyaluronic acid/resveratrol hydrogel described by Sheu *et al.* was evaluated concerning mRNA expression (collagen type I and II, MMPs) upon lipopolysaccharide (LPS) induced inflammation (Sheu *et al.*, 2013). Still, histological analysis, biochemical quantification of ECM composition, and evaluation of protein expression remained unregarded.

In another study, RSV was histologically shown to preserve proteoglycan content in full-thickness femoral cartilage explants challenged with IL-1β (Im *et al.*,

2012). Furthermore, Im *et al.* cultured articular chondrocytes in alginate beads for 21 days in the presence of RSV but absence of inflammatory mediators and assessed proteoglycan accumulation (Im *et al.*, 2012). Yet, these experiments did neither address biochemical quantification of collagen content nor expression levels of different types of collagen. In an *in vivo* animal study, RSV reduced cartilage tissue degeneration and loss of proteoglycan content in rabbits with unilateral anterior cruciate ligament transaction as surgical OA arthritic model (Wang *et al.*, 2011). Also, after conducting destabilization of the medial meniscus in mice as OA model, intra-articular injection of RSV preserved collagen type II expression and reduced expression of MMP13 (Li *et al.*, 2015).

Even though RSV is already noted in the literature, its eventual clinical use for OA patients remains unclear. This especially applies to application in cell-based therapy as long-term effects on 3D articular chondrocyte constructs cultured in an inflammatory environment with regard to tissue quality, especially composition of the ECM, have remained unexplored so far.

1.5 Goals of the thesis

Currently, OA therapies including NSAIDs and joint replacement are symptomatic and primarily address end-stage symptoms of an eventually progressing and impeding disease (Tonge *et al.*, 2014; Mobasheri, 2013). On the other hand, promising therapeutic concepts including cell-based therapy gain in importance. So far, repair and tissue engineering techniques for articular cartilage are mainly applied in posttraumatic but otherwise healthy tissue. Yet, articular cartilage in OA is additionally impaired by pro-inflammatory cytokines such as IL-1β, which has been shown to be detrimental to tissue quality (Jenei-Lanzl *et al.*, 2019). Thus, there is a strong demand for novel therapeutic concepts, such as integrating the application of anti-inflammatory agents into cartilage repair techniques in order to block long-term progression of OA already in early disease stages. Hence, in order to evaluate the applicability of RSV as a potent anti-inflammatory agent for cell-based therapies, in the present study the potential of RSV to maintain construct quality, especially ECM composition, under long-term inflammatory conditions was investigated. Specifically, 3D porcine articular chondrocyte pellet constructs were analyzed in a long-term culture set-up of 14 days employing the inflammatory cytokine IL-1β. Pellets were cultured either with IL-1β alone, both IL-1β and RSV, or RSV alone. In addition to that, experiments with an extra preculture in a non-inflammatory milieu for 7 days prior to the 14-day culture period with treatments were performed. Besides quantitative biochemical assays, histological and immunohistochemical analyses of ECM composition as well as quantitative real-time polymerase chain reaction (qRT-PCR) analyses were conducted. The defining question of the presented study was the impact of RSV on both quantity and, regarding different types of collagen, quality of synthesized ECM of IL-1β-challenged chondrocyte constructs in long-term cultures.

Part II

Materials and Methods

Chapter 2

Materials

2.1 Instruments

Table 2.1: Overview of instruments.

Instrument	Manufacturer	Main branch
Accu-jet® pro	Brand	Wertheim, Germany
Analytical scale	Ohaus	Zurich, Switzerland
Analytical scale XA 105	Mettler-Toledo	Columbus, USA
Centrifuge Rotina 420 R	Hettich	Tuttlingen, Germany
Centrifuge SIGMA 1-14	SIGMA Laborzentrifugen GmbH	Osterode, Germany
Centrifuge Heraeus® Multifuge® 3 S-R	Thermo Scientific	Waltham, USA
CO_2 incubator	IBS Integra Biosciences	Fernwald, Germany
Cryostat CM 3050S	Leica	Wetzlar, Germany
Hemacytometer Neubauer	Paul Marienfeld GmbH	Lauda, Germany
Laminar flow box Typ-HS18	Heraeus	Hanau, Germany
Orbital shaker Unimax 1010	Heidolph	Schwabach, Germany
Mastercycler® Gradient	Eppendorf	Hamburg, Germany
Magnetic stirrer	VWR	Darmstadt, Germany
Microscope BX51 and camera DP71	Olympus	Hamburg, Germany
Microscope camera DigiMicro Profi	DNT	Dietzenbach, Germany

Instrument	Manufacturer	Main branch
Microscope IX51 and camera XC30	Olympus	Hamburg, Germany
NanoDrop 2000c	Thermo Scientific	Waltham, USA
pH-meter HI2210	Hanna Instruments	Kehl am Rhein, Germany
Pipettes Research® Plus	Eppendorf	Hamburg, Germany
Real-Time PCR Detection System CFX96T™	Bio-Rad	Munich, Germany
Tecan Infinite M200 Pro	Tecan	Crailsheim, Germany
Thermomixer comfort MTP	Eppendorf	Hamburg, Germany
Thermomixer MHR 23	DITABIS	Pforzheim, Germany
Vortex, IKAR MS3 basic	IKAR	Staufen, Germany
Water bath	Memmert	Schwabach, Germany

2.2 Consumables

Table 2.2: Overview of used consumables.

Consumable	Manufacturer	Main branch
Bottle top-filter Nalgene®	Thermo Scientific	Waltham, USA
Coverslip 24 x 60 mm	MENZEL	Braunschweig, Germany
Cryovials CryoPure 2.0 mm	Sarstedt	Nümbrecht, Germany
Dispenser tips	nerbe plus	Winsen, Germany
Disposable forceps ratiomed®	Megro GmbH	Wesel, Germany
Falcon cell strainers 100 µm	BD Biosciences	Heidelberg, Germany
Filter paper	Hartenstein	Würzburg, Germany

Consumable	Manufacturer	Main branch
Hardshell PCR plates, 96-well, thin wall	Bio-Rad	Munich, Germany
Microseal® 'C' Film	Bio-Rad	Munich, Germany
Microtome blades	Feather	Osaka, Japan
96-well plate	TPP	Trasadingen, Switzerland
96-well plate (conical bottom)	TPP	Trasadingen, Switzerland
96-well plate black	Thermo Scientific	Waltham, USA
Parafilm	Pechiney	Chicago, USA
PAP pen liquid blocker	Sigma-Aldrich	Munich, Germany
PCR-strips 8 tubes 0.2 mL	Carl Roth GmbH	Karlsruhe, Germany
Pipette filter tips	Sarstedt	Nümbrecht, Germany
Pipette tips	Starlab	Hamburg, Germany
Pipettes serological	Greiner Bio-One	Frickenhausen, Germany
Polypropylene Tubes 15 mL/50 mL	Greiner Bio-One	Frickenhausen, Germany
SafeSeal micro tubes 1.5 mL / 2.0 mL	Sarstedt	Nümbrecht, Germany
SafeSeal micro tubes 5.0 mL	nerbe plus	Winsen, Germany
Scalpels	Feather	Osaka, Japan
Single-edged razor blades	GEM/Personna	Verona, USA
SuperFrost™ plus glass slide	R. Langenbrinck	Emmendingen, Germany
Syringe Filter Minisart® 0.2 µm	Sartorius AG	Göttingen, Germany

Consumable	Manufacturer	Main branch
Syringes	BD Biosciences	Heidelberg, Germany
Syringes Omnican40	B. Braun	Melsungen, Germany
Tissue culture flasks T75/T175	Greiner Bio-One	Frickenhausen, Germany

2.3 Chemicals

Table 2.3: Overview of used chemicals.

Chemical	Manufacturer	Main branch
Ambion RNaseZAP	Life Technologies	Karlsruhe, Germany
Antibody diluent, Dako REAL™	Dako	Hamburg, Germany
Aqua ad iniectabilia	B. Braun	Melsungen, Germany
Ascorbic acid-2-phosphate	Sigma-Aldrich	Munich, Germany
Brilliant III Ultra-Fast SYBR® Green QPCR Master Mix	Agilent	Santa Clara, USA
DAPI mounting medium ImmunoSelect®	Dako	Hamburg, Germany
DNase I	Roche	Basel, Swiss
Distilled water (DNase/RNase free)	Life Technologies	Karlsruhe, Germany
Dulbecco's phosphate-buffered saline (PBS)	Life Technologies	Karlsruhe, Germany
Dulbecco's Modified Eagle's Medium (DMEM)	Sigma-Aldrich	Munich, Germany
Entellan®	Merck	Darmstadt, Germany
Fetal Bovine Serum (FBS)	Invitrogen	Karlsruhe, Germany
Hematoxylin	Bio Optica	Milan, Italy
HEPES buffer	Sigma-Aldrich	Munich, Germany
Hoechst 33258 dye	Polysciences	Warrington, USA
ImProm-II™ Reverse Transcription System Kit	Promega	Madison, USA
Interleukin-1β (IL-1β)	BioLegend	London, UK
ITS+ Premix	Corning	NY, USA

Chemical	Manufacturer	Main branch
MESA GREEN qPCR MasterMix Plus for SYBR® Assay	Eurogentec	Seraing, Belgium
Non-essential amino acids (NEAA)	Thermo Scientific	Waltham, USA
Papain	Worthington	Lakewood, USA
Phosphate-buffered saline (PBS) (Dulbecco A)	Thermo Scientific	Waltham, USA
Penicillin-streptomycin	Invitrogen	Karlsruhe, Germany
Phosphate-buffered saline (PBS) (Dulbecco A) tablets	Thermo Scientific	Waltham, USA
Proline	Sigma-Aldrich	Munich, Germany
Proteinase K (Digest-All 4)	Life Technologies	Karlsruhe, Germany
Resveratrol (RSV)	Sigma-Aldrich	Munich, Germany
Sodium pyruvate	Sigma-Aldrich	Munich, Germany
Terralin Liquid® disinfectant	Schülke	Norderstedt, Germany
Tissue-Tek® O.C.T. compound	Sakura Finetek	Zoeterwonde, Netherlands
TRIzol® reagent	Life Technologies	Karlsruhe, Germany
Tween® 20	Applichem	Darmstadt, Germany
Trypsin-EDTA 0.25 %	Life Technologies	Karlsruhe, Germany
Type II Collagenase	Worthington	Lakewood, USA

2.4 Antibodies

Table 2.4: Overview of used antibodies.

Antibody	Type/Source	Dilution	Manufacturer
Anti-Aggrecan	Monoclonal IgG mouse 969D 4D11 2A9	1:300	Thermo Scientific
Anti-Collagen I	Monoclonal IgG mouse ab6308	1:600	Abcam
Anti-Collagen II	Polyclonal IgG rabbit ab34712	1:200	Abcam
Anti-Collagen X	Monoclonal IgG mouse CloneX53	1:50	eBioscience
Anti-MMP13	Polyclonal IgG rabbit ab39012	1:100	Abcam
Alexa Fluor® 488 Goat Anti-Mouse	Polyclonal IgG goat (115-545-146)	1:100	Jackson Immuno Research
Cy™3 Goat Anti-Rabbit	Polyclonal IgG goat (111-165-003)	1:100	Jackson Immuno Research
IgG1 negative control	Polyclonal IgG mouse	According to primary antibody concentration	Dako (X0931)
IgG1 isotype control	Polyclonal IgG rabbit	According to primary antibody concentration	Dianova Clone pAK (DLN-13121)

2.5 Primers

Table 2.5: Overview of used primers.

Gene	Primer Sequence	
Aggrecan	forward	AGACAGTGACCCTGAC
	reverse	CCAGGGGCAATAAAGG
Collagen I	forward	CCAACAAGGCCAAGAAGAAG
	reverse	ATGGTACCTGAGGCCGTTCT
Collagen II	forward	GCACGGATGGTCCCAAAG
	reverse	CAGCAGCTCCCCTCTCAC
Collagen X	forward	CACCAAGGCACAGTTCTTCA
	reverse	ACCGGGAATACCTTGCTCTC
MMP13	forward	TTGATGATGATGAAACCTGGA
	reverse	ACTCATGGGCAGCAACAAG
Actb (β-Actin)	forward	AAGCCAACCGTGAGAAGATG
	reverse	GTACATGGCTGGGGTGTTG

2.6 Cell culture media

Table 2.6: Overview of used cell culture media.

Medium	Composition
Expansion medium	Dulbecco's Modified Eagle's Medium (DMEM high glucose, Sigma-Aldrich) supplemented with 10 % fetal bovine serum (FBS) and 1% penicillin-streptomycin (100 U/ml penicillin, 0.1 mg/ml streptomycin).
Seeding medium	DMEM high glucose supplemented with 1% penicillin-streptomycin, 50 µg/mL ascorbic acid-2-phosphate, 40 µg/mL proline, 10 mM HEPES, 0.1 mM non-essential amino acids and 10% FBS.
Chondrocyte medium	DMEM high glucose supplemented with 1 % penicillin-streptomycin, 50 µg/mL ascorbic acid-2-phosphate, 40 µg/mL proline, 100 µg/mL sodium pyruvate and 1 % ITS+ Premix.

2.7 Buffers and solutions

Table 2.7: Overview of used buffers and solutions.

Buffer / Solution	Composition
Blocking solution (IHC)	1.5 % BSA dissolved in PBS.
Buffered formalin	3.7 % formalin (37 % stock solution) diluted in PBS.
Chloramine T solution	70.5 mg chloramine T, 4 mL citric acid buffer, and 0.5 mL 2-propanol.
Collagenase buffer	0.1 M HEPES, 0.12 M NaCl, 0.05 M KCl, 0.001 M $CaCl_2$ and 0.005 M glucose dissolved in ddH_2O. Adjust to pH 7.4 and store at 4 °C. For digestion freshly add 10 % FBS and 0.15 % type II collagenase. Sterilize with a 0.2 µm bottle top-filter.
DAB solution	750 mg p-dimethylamino-benzaldehyde (DAB), 3 mL 2-propanol, and 1.3 ml 60 % perchloric acid.
DMMB solution	16 mg dimethylmethylene blue (DMMB) is dissolved in 5 mL absolute ethanol for 16 h and subsequently added to NaCl-glycine solution consisting of 3.04 g glycine, 2.37 g NaCl and 900 ml ddH_2O. Adjust to pH 3.0 with HCl 32 %.
Hoechst 33258 stock solution	2 mg/mL is dissolved in ddH_2O.
Papain digestion buffer	20 mL PBE buffer, 17 mg L-cysteine, 3 U/mL papain. For sterilization a 0.2 µm syringe-filter was used.

Buffer / Solution	Composition
PBE buffer	6.53 g Na_2HPO_4, 6.48 g NaH_2PO_4, 10 mL 500 mM EDTA and 900 mL ddH_2O. Adjust to pH 6.5, add ddH_2O to 1 L volume and sterilize with a 0.2 µm filter.
PBS	10 PBS (Dulbecco A) tablets dissolved in 1 L ddH_2O.
TBS	0.1 M NaCl, 1 mM EDTA and 10 mM Tris dissolved in ddH_2O. Adjust to pH 7.4.
TBST	0.1 % Tween® 20 in 1 x TBS.

2.8 Software

Table 2.8: Overview of used software.

Software/Version	Manufacturer	Main branch
CellSense™ 1.16	Olympus	Hamburg, Germany
Graphpad Prism Version 6.0	GraphPad Software	La Jolla, USA
Microsoft Office 2018	Microsoft	Redmond, USA

Chapter 3

Methods

3.1 Isolation of chondrocytes and culture of cells

Articular cartilage was separated from porcine femorotibial joints of 4-5 months old animals sourced from a local butcher within few hours after slaughter. Thereby, a lateral capsulotomy was performed to open the joint and subsequently remove cartilage from the underlying bone. In order to prevent contamination, surgical instruments were disinfected with ethanol and tissue explants were washed with phosphate-buffered saline (PBS) containing 1 % penicillin-streptomycin. Slices were chopped into pieces of approximately one-millimeter size and then digested with type II collagenase as described earlier (Blunk *et al.*, 2002; Kellner *et al.*, 2001).

In order to wash off remaining collagenase, the suspension was centrifuged (300 g, 10 min) and resuspended in PBS. After another centrifugation and washing in PBS the formed cell pellet was resuspended in expansion medium consisting of DMEM high glucose 4.5 g/L complemented with 10 % fetal bovine serum and 1% penicillin-streptomycin. In order to estimate the number of isolated vital cells, trypan blue staining and a Neubauer counting chamber were used. Subsequently, cells were cultured in T175 cm^2 culture flasks at 37 °C, 5 % CO_2, 21 % O_2 with a density of 15000 cells per cm^2. Medium change was conducted every 48 hours until cells reached 90 % confluence after five days and non-adherent cells were removed by washing with PBS carefully at every change of medium. Chondrocytes were passaged applying trypsin-EDTA at 0.25 %.

Therefore, cells were incubated with trypsin-EDTA for 5 min at 37 °C and trypsinization was stopped by adding an equivalent amount of expansion medium. After centrifugation (300 g, 10 min) and resuspension in seeding medium obtained first passage cells (P1) were used in the experiments.

3.2 Production of pellet constructs

Chondrocytes (P1) were suspended in seeding medium comprising DMEM high glucose, 10% FBS, 1% penicillin-streptomycin, 50 µg/mL ascorbic acid-2-phosphate, 40 µg/mL proline, 10 mM HEPES, and 0.1 mM non-essential amino acids. Cells were seeded at a quantity of $2x10^5$ cells per well in 96-well plates (conical bottom) followed by centrifugation at 300 g for 5 min (Heraeus® Multifuge® 3 S-R) and subsequent incubation overnight in an incubator (37 °C, 5 % CO_2, 21 % O_2) in order to enable dense cell pellet formation. Finally, pellets were cultured in chondrocyte medium consisting of DMEM high glucose, 1 % penicillin-streptomycin, 50 µg/mL ascorbic acid-2-phosphate, 40 µg/mL proline, 100 µg/mL sodium pyruvate, and 1 % insulin-transferrin-selenium-plus (ITS+ Premix).

3.3 Experimental design

In order to simulate an inflammatory environment, pellets cultured in chondrocyte medium were treated with IL-1β at concentrations of either 1 ng/ml or 10 ng/ml. In a third group constructs received both inflammatory IL-1β at 10 ng/ml and RSV at 50 μM as an anti-inflammatory stimulus. A further group received RSV only in order to assess effects on pellets under non-inflammatory

conditions. Pellets treated with chondrocyte medium only served as control. In one set of experiments pellets received treatments immediately for 14 days, labelled as 'w/o preculture' (Figure 3.1). In contrast, pellets in a second set were initially matured for 7 days before cultivation with treatments for 14 days, labelled as 'with preculture'. Within the preculture period they either received chondrocyte medium only, seeding medium containing FBS (10%) or chondrocyte medium supplemented with RSV (50 μM) (Figure 3.1).

Out of these different set-ups, the precultivation with only chondrocyte medium represented the main study, enabling construct maturation without additional influences. Further set-ups adding FBS and RSV, respectively, were carried out to generate matured and preconditioned constructs, enabling investigations into effects of these agents in preculture concerning construct quality under modified starting conditions.

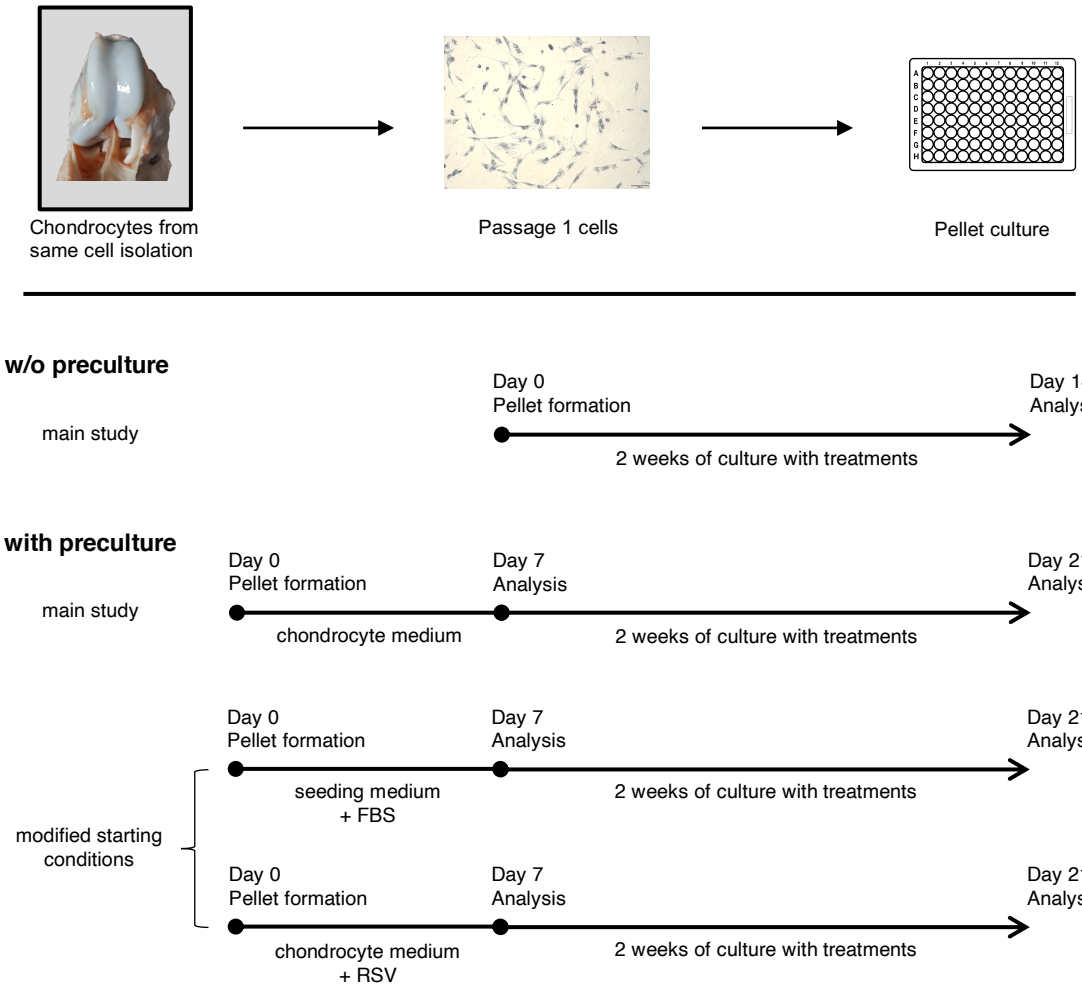

Figure 3.1. Experimental design: porcine articular chondrocytes were isolated, passaged, and pellets were formed. In one set, pellets immediately received treatments for 14 days in chondrocyte medium, whereas in a second set they were initially matured for 7 days before cultivation with treatments for 14 days in chondrocyte medium. Within the preculture period they received either chondrocyte medium only, representing the main study, or seeding medium containing FBS (10%) or chondrocyte medium supplemented with RSV (50 μM) as modified starting conditions.

3.4 Biochemical analyses

3.4.1 Papain Digestion

With regard to biochemical analyses, 9 pellets per experimental group were used, of which 3 per sample were pooled, resulting in n=3. Subsequently, pellets were washed with PBS and then suspended in 0.375 mL papain solution at 3 U/ml for 16 h at 60 °C in 2 ml SafeSeal micro tubes for enzymatic digestion (Böck *et al.*, 2018). The digested samples were stored at -18 °C until used.

3.4.2 DNA Assay

Hoechst 33258 dye was used for measurement of DNA content. Therefore, 10 µL of papain digested samples were incubated in 200 µL of a Hoechst 33258 dye solution. A fluorimeter (Infinite® M200 PRO) was utilized at an excitation wavelength of 360 nm and an emission wavelength of 460 nm for quantitative analysis (Kim *et al.*, 1988).

3.4.3 GAG Assay

Samples were incubated with dimethylmethylene blue dye (DMMB) in order to determine sulphated glycosaminoglycan (GAG) content (Farndale *et al.*, 1986). Therefore, 10 µL of papain digested samples and 40 µL of PBE-cysteine buffer were added to 200 µL DMMB solution and measured spectrophotometrically with the Infinite® M200 PRO at 525 nm, while chondroitin sulphate served as standard.

3.4.4 Collagen Assay

After hydrolysis with hydrochloric acid and reaction with chloramine-T and p-dimethylaminobenzaldehyde (DAB), hydroxyproline content of pellets was measured (Woessner, 1961). Therefore, 10 µL of papain digested samples were added to 100 µL of 36 % HCl and hydrolyzed for 16 h at 105 °C. Subsequently, HCl was let to evaporate in a fume cupboard for 2 h at 105 °C and residual material was resuspended in 500 µL ddH_2O. For measurement, 50 µL chloramine-T solution and 50 µL DAB solution were incubated with 100 µL of ddH_2O resuspended samples for 30 min at 65 °C. Quantification was performed with a spectrophotometer at 560 nm (Rosano *et al.*, 1987), using L-hydroxyproline as standard. To calculate total collagen content, a hydroxyproline to collagen ratio of 1:10 was used (Hollander *et al.*, 1994).

3.5 Cryosectioning

The pellets were removed from chondrocyte medium, washed with PBS for 10 min and then fixed in 3.7 % PBS buffered formalin for 60 min. After washed again in PBS for 10 min constructs were transmitted into cryomolds and incubated in O.C.T. overnight at 4 °C. After 18 h cryomolds including O.C.T-embedded pellets were frozen with liquid nitrogen and stored at -18 °C until used. For sectioning of the frozen constructs, a Cryostat CM 3050S was used at -20 °C. Thereby, 5 µm longitudinal sections were cut, collected on Super Frost® plus glass slides and stored at -18 °C until stained.

3.6 Histology and Immunohistochemistry (IHC)

3.6.1 Histology

Pellets were fixed in 3.7% buffered formalin and imbedded in Tissue-Tek O.C.T. Compound for histological and immunohistochemical analyses. As described previously, samples were sliced into 5 µm-thick sections and assembled on Super Frost® plus glass slides (Stichler *et al.*, 2017). In order to evaluate GAG deposition histologically, sections were hydrated for 1 min, then immersed in Weigert's hematoxylin for 5 min, followed by washing under running tap water for 5 min, counter-staining in 0.02 % fast green for 4 min, 1 % acetic acid for 10 sec, and 0.1 % safranin O for 6 min. After dehydration in a rising alcohol series and incubation in xylene for 2 min sections were mounted with Entellan® and stored at room temperature until images were taken with a microscope (Microscope BX51 plus DP71 camera).

3.6.2 Immunohistochemistry

To ensure antigen retrieval for immunohistochemical analyses, rehydrated sections were immersed in Proteinase K for 10 min. Sections were washed three times for 3 min with Tween 20 in Tris-buffered saline (TBST) (Pietkiewicz *et al.*, 2018) and then blocked with 1 % bovine serum albumin (BSA) in PBS for 20 min. Primary antibodies were dissolved in antibody diluent (Dako REAL™), and incubated overnight at the following dilutions: For MMP13 (polyclonal IgG rabbit ab39012) at 1:100, for collagen type I (monoclonal IgG mouse ab6308) at 1:600, for collagen type II (polyclonal IgG rabbit ab34712) at 1:200, and for

collagen type X (monoclonal IgG mouse CloneX53) at 1:50. Subsequently, sections were washed three times in TBST for 3 min. Secondary antibodies Cy™3 goat anti-rabbit (111-165-003) at 1:100 or Alexa Fluor® 488 goat anti-mouse (115-545-146) at 1:100 were diluted and incubated for 2 hours in the darkness. After that, slides were mounted with DAPI mounting medium ImmunoSelect®. Identical concentrations of species-matched immunoglobins on equally treated sections were used as negative controls. For imaging, a fluorescence microscope (Microscope BX51/DP71 camera) was used.

3.6.3 Evaluation of absolute pellet diameter

Microscope BX51 plus DP71 camera and CellSense™ 1.16 software were used to determine pellet size by imaging and measurement. For each group, samples (n=3) were measured for absolute diameter six-fold using a different starting point each time. Mean values were applied for statistical analyses.

3.7 RNA isolation and qRT-PCR analysis

For RNA isolation, pellets were pooled (2 per sample, with n=3) and homogenized in TRIzol® reagent and total RNA was extracted as indicated by the manufacturer. The ImProm™ reverse transcription system kit was used to perform transcription into first strand complementary DNA (cDNA). Quantitative real-time polymerase chain reaction (qRT-PCR) analysis was executed with the Real-Time PCR Detection System CFX96T™ utilizing the Brilliant III Ultra-Fast SYBR® Green QPCR Master Mix with primer pairs for collagen type I, collagen type II, collagen type X, aggrecan, and beta-actin (Actb)

as housekeeping gene as stated in Table 2.5. (Gredes, 2008; customized by biomers.net GmbH, Ulm, Germany). The subsequent cycling protocol was applied for all primers: 95°C for 3 min followed by 40 cycles at 95 °C for 5 sec and 60 °C for 30 sec, concluded by an increase in temperature from 65 °C to 95 °C in 0.5 °C increments with 5 sec per step. The mRNA expression levels of all genes were normalized to the housekeeping gene beta-actin for each group.
The $2^{-\Delta\Delta CT}$ method was used to assess the increase in expression levels for each gene. Further, values were normalized to the control group receiving chondrocyte medium only.

3.8 Statistical analysis

Statistical analysis was executed using GraphPad Prism, Version 6.0. Data are displayed as mean values ± standard deviation (SD). Statistical significance between groups was evaluated by two-way analysis of variance (ANOVA) and subsequent Tukey's post-hoc test. Values of $p < 0.05$ were regarded statistically significant and significant differences were labeled as follows: $^{***}p<0.001$, $^{**}p<0.01$, $^{*}p<0.05$, and $^{\Delta\Delta\Delta}p<0.001$, $^{\Delta\Delta}p<0.01$, respectively.

Part III

Results

Chapter 4

Results

4.1 Effects of IL-1β and RSV on pellet size and DNA content

Culture of pellet constructs was conducted in chondrocyte medium (Figure 4.1) and treatments were supplemented as follows: IL-1β (1 or 10 ng/ml), both IL-1β (10 ng/ml) and RSV (50 μM), or RSV (50 μM) alone for 14 days; cultures in only chondrocyte medium were regarded as control (Figure 4.1).

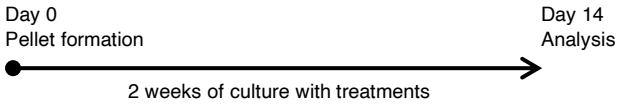

Figure 4.1. Experiments without preculture: Pellets immediately received treatments for 14 days in chondrocyte medium.

Treatment with IL-1β at 10 ng/ml, in comparison to controls, resulted in a significantly smaller pellet size and reduced DNA content (Figure 4.2.A). Contrary, treatment with IL-1β at 1 ng/ml led to only a slight decrease in pellet size and no significant change in DNA content compared to controls. RSV counteracted the IL-1β-induced decrease in both pellet size and DNA content, i.e., it significantly enhanced diameter and DNA content (IL-1β: 1.45±0.11 µg, IL-1β+RSV: 3.06±0.10 µg DNA; $p<0.001$) even up to control levels (Ctrl: 3.24±0.22 µg DNA) (Figure 4.2.A).

4.2 RSV counteracts IL-1β-induced glycosaminoglycan depletion and MMP13 expression

In terms of GAG deposition, IL-1β at 1 ng/ml caused no significant change, whereas treatment with IL-1β at 10 ng/ml resulted in a tremendous depletion of absolute GAG content and GAG/DNA, as compared to controls (Ctrl: 92.04±8.94 µg/µg, IL-1β: 8.35±0.96 µg/µg GAG/DNA; $p<0.001$) (Figure 4.2.A). However, RSV co-treatment counteracted the inflammatory stimulus and led to a partial recovery of GAG content with significant increases in both total GAG and GAG/DNA (IL-1β: 8.35±0.96 µg/µg, IL-1β+RSV: 43.44±7.20 µg/µg GAG/DNA; $p<0.001$) (Figure 4.2.A). Interestingly, RSV alone enhanced GAG/DNA content, as compared to controls (Ctrl: 92.04±8.94 µg, RSV: 151.63±4.31 µg/µg GAG/DNA; $p<0.001$).

Histological staining affirmed the marked reduction in size and the distinct GAG depletion for pellets treated with IL-1β at 10 ng/ml (Figure 4.2.B). Also, well confirming the quantitative data, a strong enhancement of GAG content for constructs receiving both IL-1β and RSV, as compared to IL-1β only, was clearly recognizable (Figure 4.2.B).

Immunohistochemical analyses for the major cartilage-degrading enzyme MMP13 revealed a pronounced expression in IL-1β-treated (10 ng/ml) constructs, whereas, remarkably, in pellets co-treated with IL-1β and RSV no MMP13 expression was visible (Figure 4.2.C).

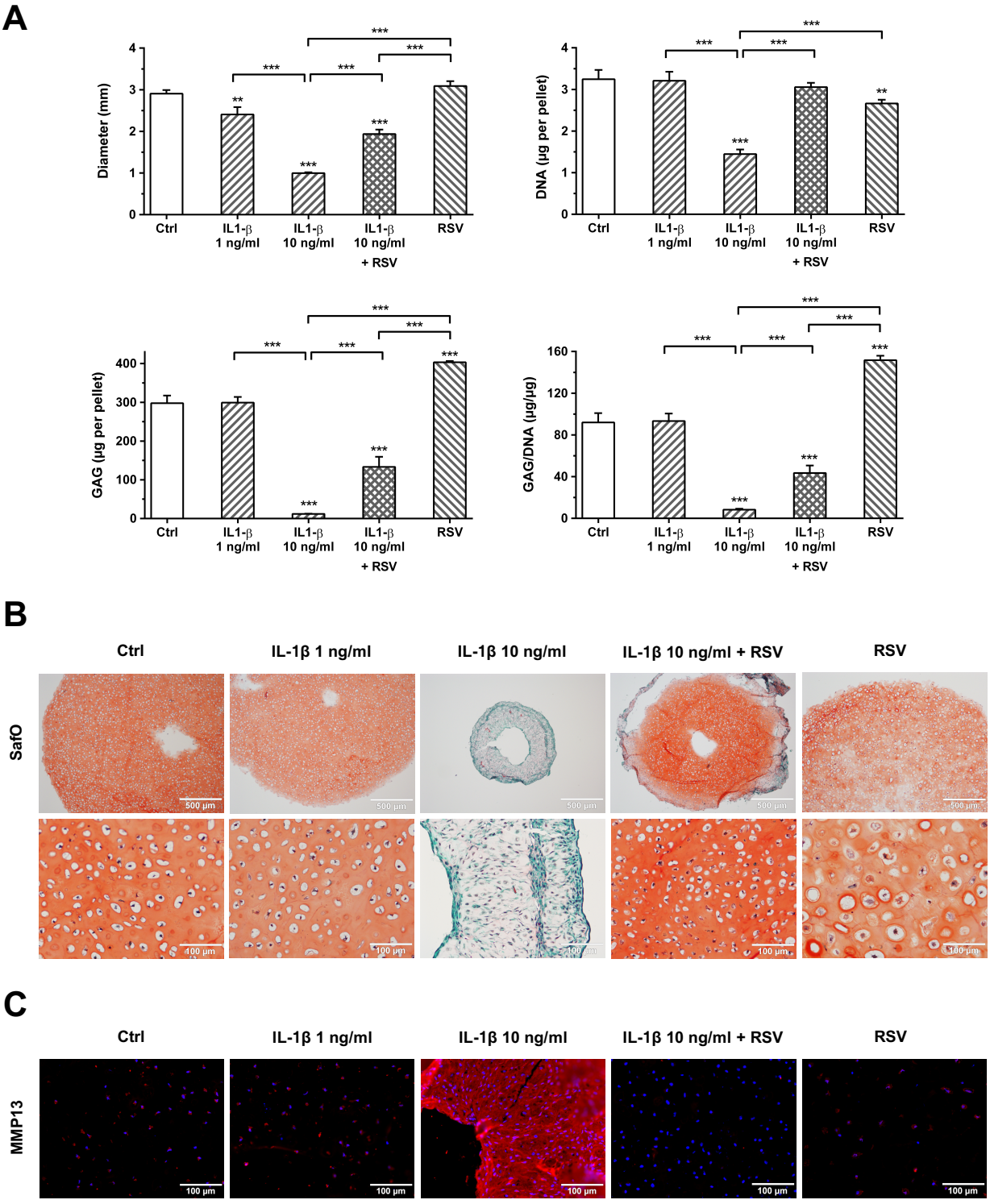

Figure 4.2. Construct analysis after 14 days of culture. (**A**) Pellet diameter and DNA content per pellet; glycosaminoglycan (GAG) deposition of chondrocytes, shown for absolute amounts of GAG (GAG/pellet) and normalized to DNA (GAG/DNA). Data are presented as means ± standard deviation (3 pellets per sample were pooled, with n=3). Asterisks above single bars represent statistical significance against control group, and above brackets between displayed groups; ***p<0.001, **p<0.01. (**B**) Histological staining for GAG deposition with safranin-O. Scale bars represent 500 μm (upper) and 100 μm (lower), respectively. (**C**) Immunohistochemical staining for MMP13. Scale bars represent 100 μm.

4.3 RSV affects collagen content and composition

Treatment with IL-1β at 10 ng/ml, as compared to controls, significantly decreased absolute quantity of total collagen (Ctrl: 86.64±7.12 µg, IL-1β: 25.29±4.58 µg collagen; $p<0.001$) and collagen/DNA content (Ctrl: 26.69±0.70 µg/µg, IL-1β: 17.38±1.90 µg/µg collagen/DNA; $p<0.001$), whereas pellets receiving IL-1β at 1 ng/ml again showed no variation to controls (Figure 4.3.A). Again, co-treatment of IL-1β-challenged constructs with RSV significantly increased absolute collagen content (IL-1β: 25.29±4.58 µg, IL-1β+RSV: 68.04±10.16 µg; $p<0.001$), whereas enhancement of collagen/DNA was not statistically significant (IL-1β: 17.38±1.90 µg/µg, IL-1β+RSV: 22.20±2.64 µg/µg collagen/DNA) (Figure 4.3.A). Immunohistochemical analyses revealed substantial collagen type II expression in all samples (Figure 4.3.B). However, concerning samples receiving RSV only, staining appeared less intense and cells in this group seemed to partly have a hypertrophic morphology. Besides, qRT-PCR analysis at day 14 indicated no significant differences in gene expression of collagen type II when standardized to the values of the control group (Figure 4.3.C). Immunohistochemical staining for collagen type I was distinctly pronounced in samples receiving IL-1β (10 ng/ml) and also observable upon co-treatment with RSV, indicating fibrous cartilage (Figure 4.3.B). Also, qRT-PCR analysis revealed a marked increase of collagen type I expression in constructs treated with IL-1β (10 ng/ml) alone (Figure 4.3.C). Interestingly, collagen type X, which occurs in hypertrophic chondrocytes, was observed in pellets receiving RSV only, but in no other group including constructs co-treated with IL-1β and RSV (Figure 4.3.B). Correspondingly, qRT-PCR analysis revealed a significant increment in collagen type X gene expression in pellets treated with RSV only (75-fold compared to controls), but in no other group including constructs co-treated with IL-1β and RSV (Figure 4.3.C).

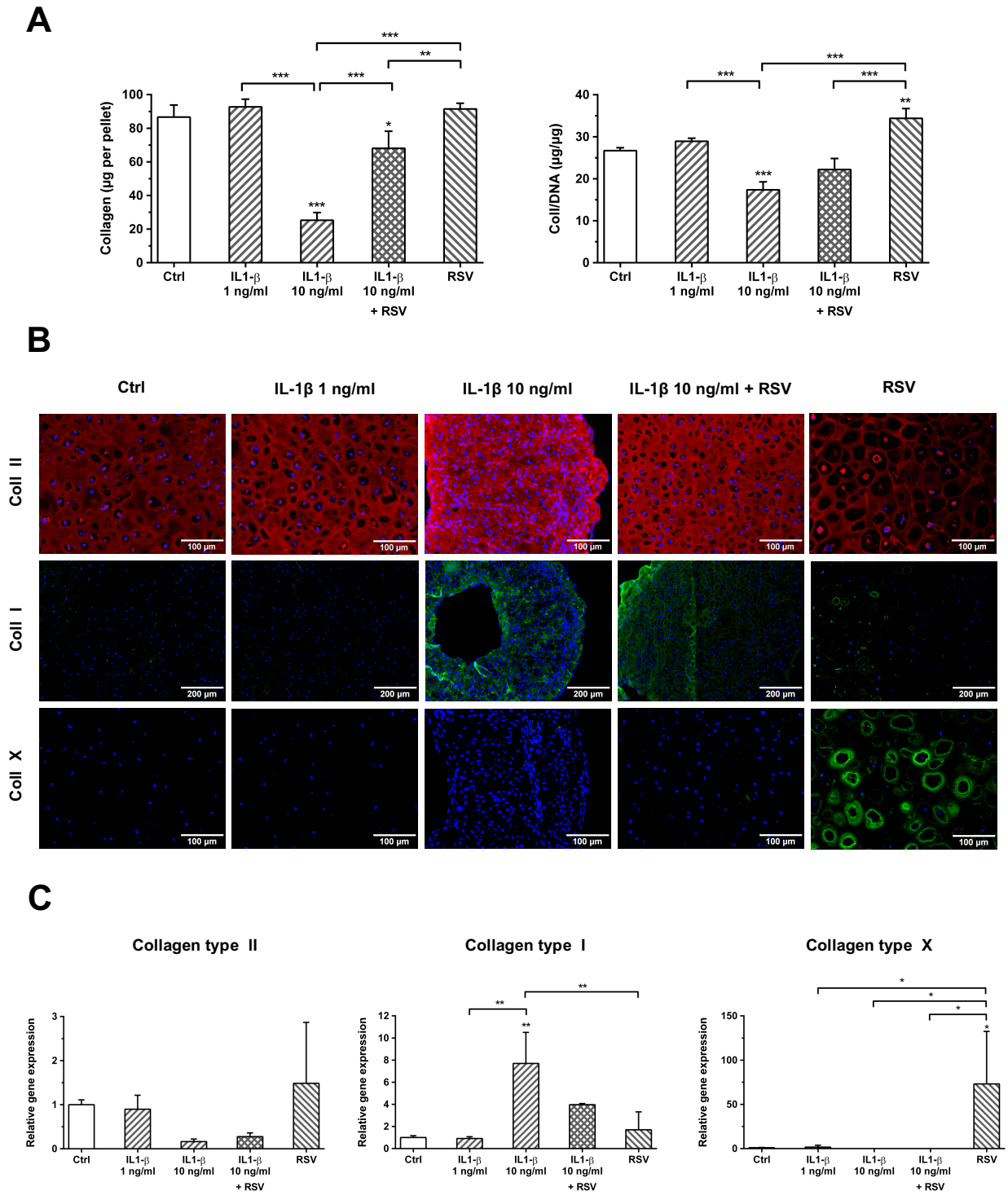

Figure 4.3. Collagen content after 14 days of culture. (**A**) Collagen production of chondrocytes, shown for absolute amounts of total collagen (collagen/pellet) and normalized to DNA (collagen/DNA). Data are presented as means ± standard deviation (3 pellets per sample were pooled, with n=3). (**B**) Immunohistochemical staining for collagen type II, type I, and type X. Scale bars represent 100 μm (upper, lower) and 200 μm (middle), respectively. (**C**) Gene expression of collagen type II, type I, and type X, quantitative real-time PCR analysis at day 14. Gene expression was normalized to beta-actin; the obtained values were further normalized to the values of the control group. Data are presented as means ± standard deviation (2 pellets per sample were pooled, with n=3). In (**A**) and (**C**), asterisks above single bars represent statistical significance against control group, and above brackets between displayed groups; ***p<0.001, **p<0.01, *p<0.05.

4.4 RSV improves IL-1β-impaired tissue composition also in the set-up with preculture

In a further experimental set-up, pellets initially received preculture in chondrocyte medium for 7 days prior to culture with treatments for 14 days in order to assess the effects of maturation on subsequent culture under inflammatory conditions (Figure 4.4).

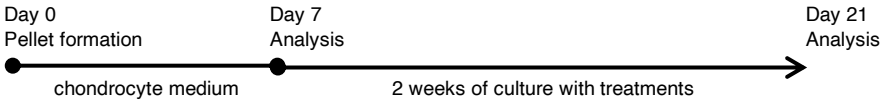

Figure 4.4. Preculture in chondrocyte medium: Pellets were initially matured for 7 days before cultivation with treatments for 14 days. Within the preculture period they received chondrocyte medium only.

After 21 days, constructs receiving IL-1β (10 ng/ml) showed significantly reduced diameter and DNA amount, as compared to controls, and did not exceed day 7 levels (IL-1β: 3.38±0.05 µg, day 7: 2.91±0.28 µg DNA) (Figure 4.5.A). Co-treatment with RSV counteracted this decrease and enhanced DNA amount up to control levels (IL-1β+RSV: 4.77±0.26 µg, Ctrl: 4.71±0.23 µg DNA) (Figure 4.5.A). In terms of absolute GAG content as well as GAG/DNA, values after 21 days for constructs receiving IL-1β (10 ng/ml) were even significantly lower than standard levels at day 7 (IL-1β: 12.24±1.05 µg/µg, day 7: 56.55±5.58 µg/µg GAG/DNA; $p<0.001$) (Figure 4.5.A). Again, co-treatment with RSV distinctly counteracted this depletion of GAG content up to control standards (IL-1β+RSV: 99.31±13.58 µg/µg, Ctrl: 89.38±7.14 µg/µg GAG/DNA) (Figure 4.5.A), whereby these results were well in accordance with histological staining (Figure 4.5.B).

Immunohistochemical staining for MMP13 revealed a slight but distinct expression in all samples, more pronounced in constructs treated with IL-1β (10 ng/ml) (Figure 4.5.C).

With regards to absolute collagen and collagen/DNA, a similar pattern as determined for GAG, although not as severe, was observed, with a moderate depletion in constructs treated with IL-1β (10 ng/ml) and again enhancement up to control standards upon co-treatment with RSV (IL-1β+RSV: 35.38±3.07 µg/µg, Ctrl: 32.95±3.10 µg/µg collagen/DNA) (Figure 4.6.A). Immunohistochemical analyses revealed abundant collagen type II expression in all samples, whereas only a slight signal at the construct periphery for collagen type I and no staining for collagen type X were detected, with no distinct variations between the groups (Figure 4.6.B).

In qRT-PCR analysis, a diminished expression of collagen type II was observed in constructs treated with IL-1β (10 ng/ml), which was enhanced up to control levels upon co-treatment with RSV. Even though qRT-PCR analysis for collagen type I at day 21 showed an upregulation for samples treated only with RSV, this trend was not depicted in immunohistochemical staining. As to collagen type X, again a markedly increased gene expression in constructs obtaining RSV only was observed (Figure 4.6.C).

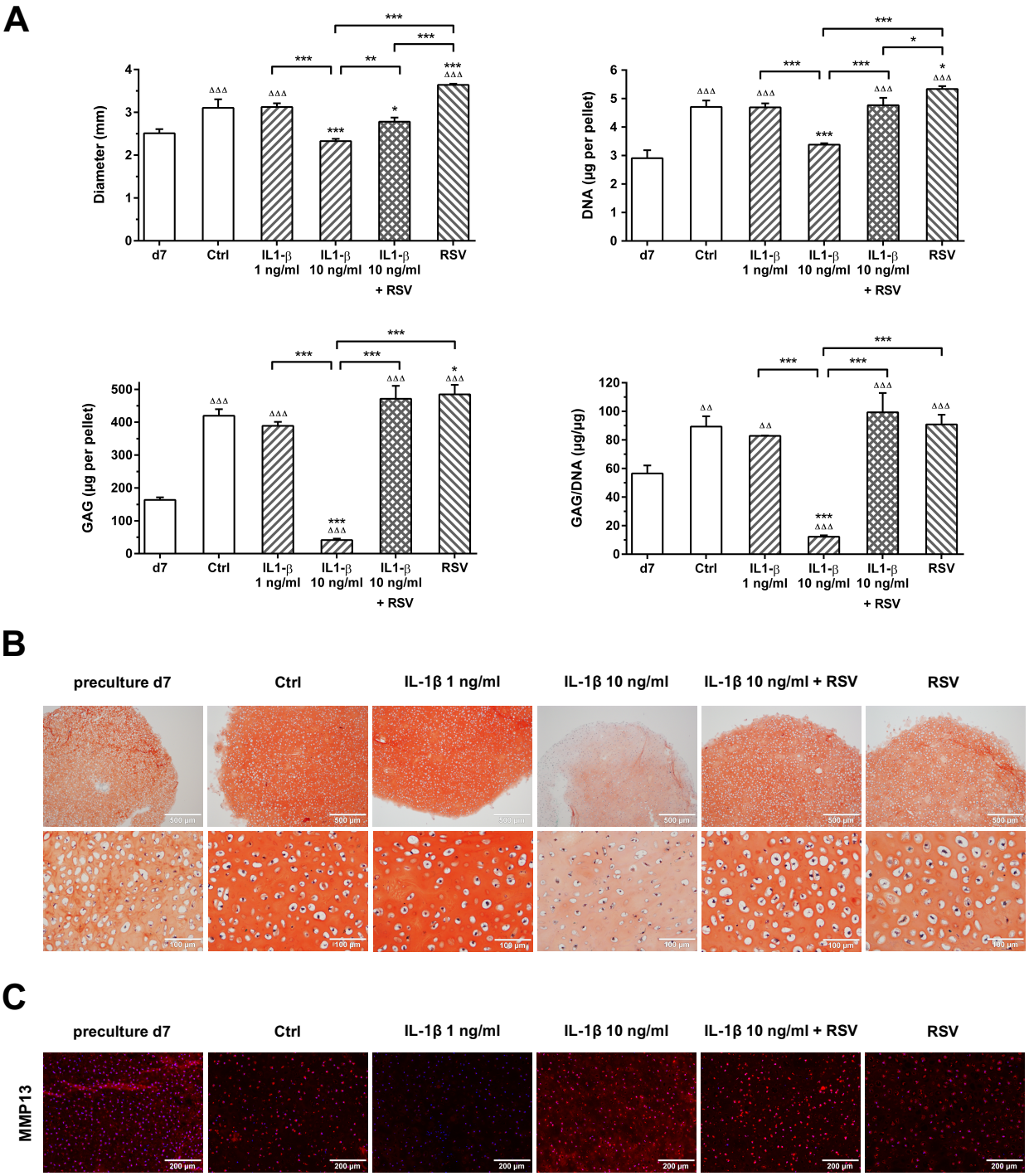

Figure 4.5. Construct analysis after 21 days of culture (7 days of precultivation in chondrocyte medium, followed by 14 days with different treatments). Data after 21 days is shown for all groups and compared to values at day 7. (**A**) Pellet diameter and DNA content per pellet; glycosaminoglycan (GAG) deposition of chondrocytes, shown for absolute amounts of GAG (GAG/pellet) and normalized to DNA (GAG/DNA). Data are presented as means ± standard deviation (3 pellets per sample were pooled, with n=3). Asterisks above single bars represent statistical significance against control group after 21 days, above brackets between displayed groups; ***p<0.001, **p<0.01, *p<0.05. Triangles above single bars represent statistical significance between the respective treatment group after 21 days and control values at day 7; $^{\Delta\Delta\Delta}$p<0.001, $^{\Delta\Delta}$p<0.01. (**B**) Histological staining for GAG deposition with safranin-O. Scale bars represent 500 μm (upper) and 100 μm (lower). (**C**) Immunohistochemical staining for MMP13. Scale bars represent 200 μm.

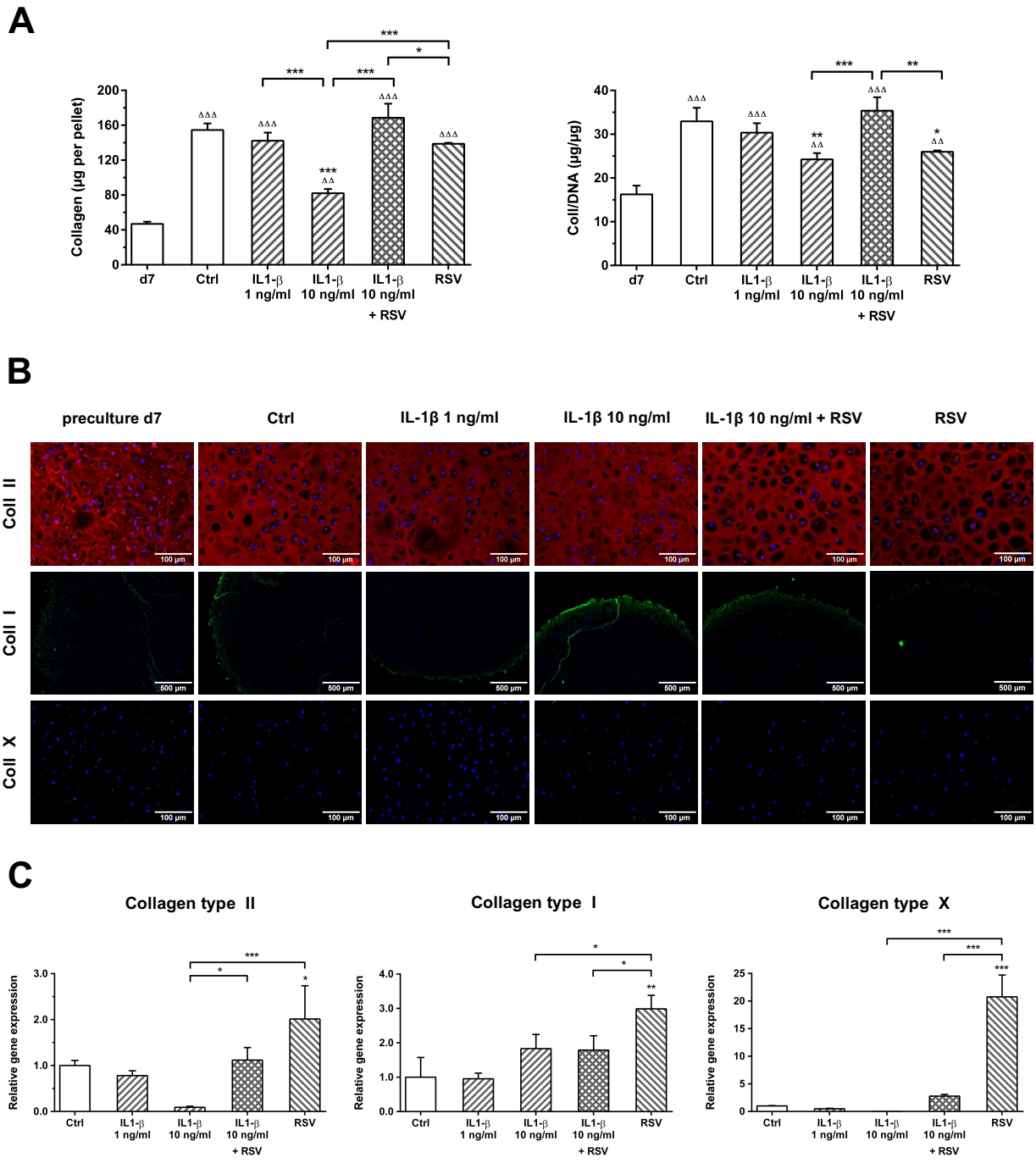

Figure 4.6. Collagen content after 21 days of culture (7 days of precultivation in chondrocyte medium, followed by 14 days with different treatments). Data after 21 days is shown for all groups and compared to values at day 7. (**A**) Collagen production of chondrocytes, shown for absolute amounts of total collagen (collagen/pellet) and normalized to DNA (collagen/DNA). Data are presented as means ± standard deviation (3 pellets per sample were pooled, with n=3). (**B**) Immunohistochemical staining for collagen type II, type I, and type X. Scale bars represent 100 μm (upper, lower) and 500 μm (middle), respectively. (**C**) Gene expression of collagen type II, type I, and type X, quantitative real-time PCR analysis at day 21. Gene expression was normalized to beta-actin; the obtained values were further normalized to the values of the control group. Data are presented as means ± standard deviation (2 pellets per sample were pooled, with n=3). In (**A**) and (**C**), asterisks above single bars represent statistical significance against control group after 21 days, above brackets between displayed groups; ***p<0.001, **p<0.01, *p<0.05. Triangles above single bars represent statistical significance between the respective treatment group after 21 days and control values at day 7; $^{\Delta\Delta\Delta}$p<0.001, $^{\Delta\Delta}$p<0.01.

4.5 Comparison of experiments without and with preculture

When directly contrasting data from the two different experimental set-ups, i.e., without and with preculture, amounts of total DNA, GAG, and collagen were significantly higher in experiments with preculture (Figure 4.7.B). Interestingly, absolute diameter of constructs receiving IL-1β at 10 ng/ml after preculture was much less affected than that of pellets without preculture (images from Figures 4.2.B and 4.5.B, directly compared in Figure 4.7.A). Similarly, upon treatment with IL-1β (10 ng/ml) a more moderate reduction in DNA and collagen content was found in the experiments including preculture. In contrast, IL-1β treatment caused a distinct decline in total GAG and GAG/DNA in both experimental set-ups (data from Figures 4.2.A and 4.5.A, directly compared in Figure 4.7.B). Interestingly, while a partial increase in GAG content upon RSV co-treatment was determined in the set-up without preculture, even a complete rescue of total GAG and GAG/DNA upon RSV co-treatment was observed in the experiments with preculture (Figure 4.7.B).

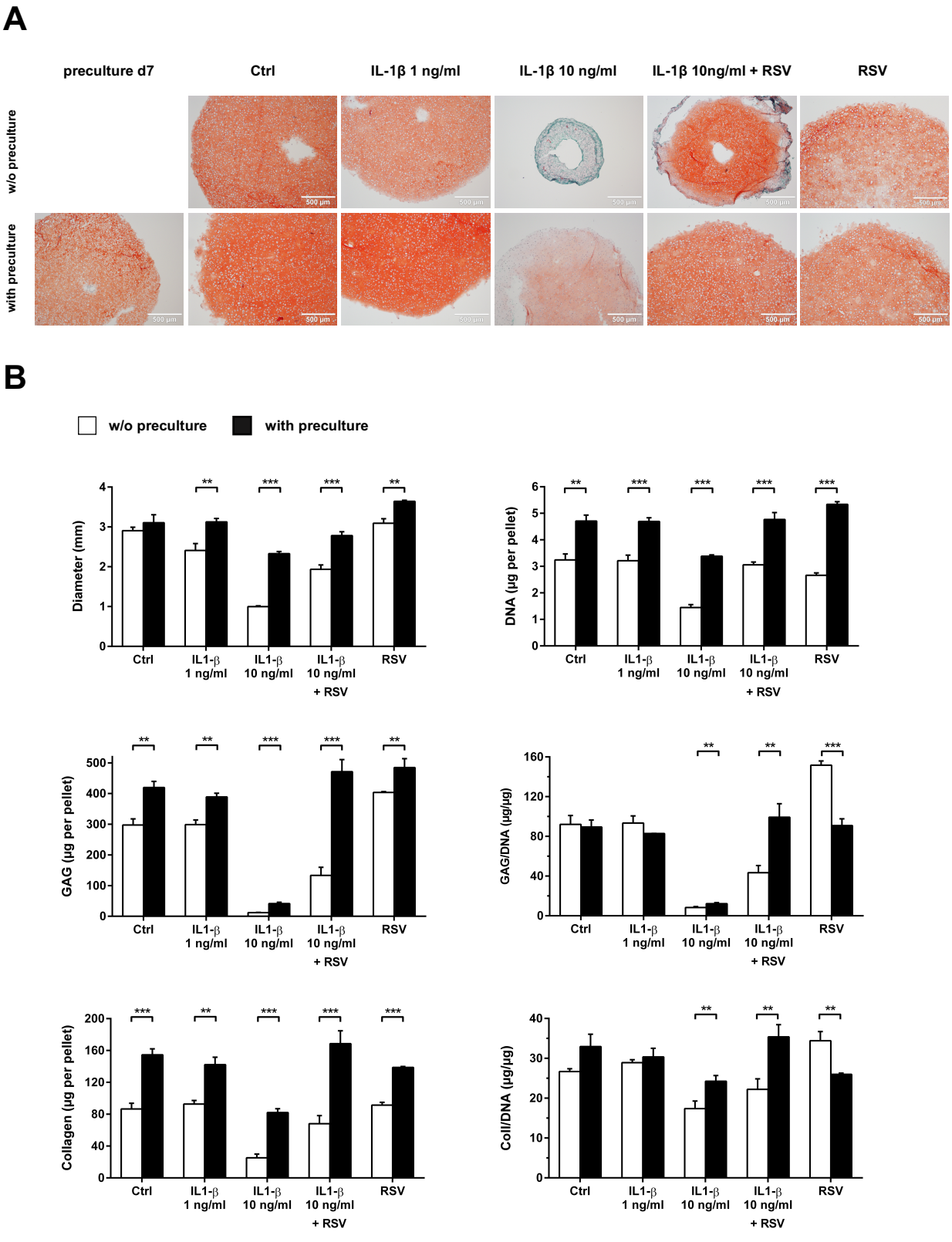

Figure 4.7. Comparison of experiments 'without (w/o) preculture' and 'with preculture'. (**A**) Histological staining for GAG deposition with safranin-O. Scale bars represent 500 μm. (**B**) Comparison of experiments 'without (w/o) preculture' and 'with preculture'. Asterisks above brackets represent statistical significance between displayed groups; ***p<0.001, **p<0.01.

4.6 Preculture under modified starting conditions

4.6.1 Preculture with FBS

In another set of experiments pellet constructs were initially precultured in seeding medium containing FBS (10%) for 7 days prior to culture with treatments for 14 days in order to evaluate the impact of FBS on subsequent culture in an inflammatory milieu (Figure 4.8).

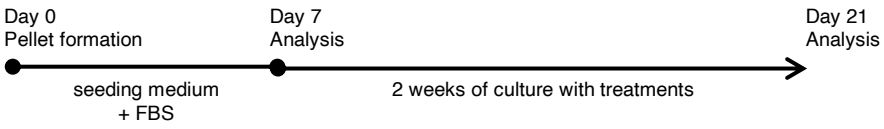

Figure 4.8. Preculture with FBS: Pellets were initially matured for 7 days before cultivation with treatments for 14 days. Within the preculture period they received seeding medium containing FBS (10%).

Regarding the preculture with 10 % FBS, treatment with IL-1β at 10 ng/ml likewise led to a significantly lower DNA content, as compared to baseline levels at day 7 (IL-1β: 0.97±0.09 µg, day 7: 1.63±0.06 µg DNA; $p<0.01$) (Figure 4.9.B), whereas treatment with IL-1β at 1 ng/ml showed no significant difference in DNA content. Again, RSV counteracted the IL-1β-induced reduction of absolute DNA amount in a highly inflammatory milieu (IL-1β: 0.97±0.09 µg, IL-1β+RSV: 1.51±0.22 µg DNA; $p<0.01$) (Figure 4.9.B).

Surprisingly, with regard to GAG deposition, treatment with IL-1β at 1 ng/ml resulted in a significantly higher absolute GAG content, as compared to controls (Ctrl: 56.19±4.35 µg, IL-1β: 76.90±9.25 µg GAG; $p<0.01$), which was further supported by histological analysis (Figure 4.9.A), but not significant when GAG

content was normalized to DNA. However, treatment with IL-1β at 10 ng/ml drastically reduced GAG/DNA (Ctrl: 31.79±1.92 µg/µg, IL-1β: 8.30±0.99 µg/µg GAG/DNA; $p<0.001$), and values were again even significantly lower than baseline level at day 7 (IL-1β: 8.30±0.99 µg/µg, day 7: 21.77±1.30 µg/µg GAG/DNA; $p<0.01$). Co-treatment with RSV likewise counteracted this loss of GAG content, however in this set-up not up to control levels (IL-1β: 8.30±0.99 µg/µg, IL-1β+RSV: 20.38±3.95 µg/µg GAG/DNA; $p<0.05$) (Figure 4.9.B).

A similar pattern as observed for GAG was determined for absolute collagen. Except for IL-1β-treated (10 ng/ml) constructs, pellets in every other group exceeded day 7 values in terms of total collagen content. Thereby, values for total collagen in the IL-1β (10 ng/ml) plus RSV co-treated group were significantly higher than of that only receiving the highly inflammatory stimulus (IL-1β at 10 ng/ml) (IL-1β: 14.05±1.43 µg, IL-1β+RSV: 23.01±1.01 µg collagen; $p<0.001$). Yet, there was no significant difference between any treatment groups when absolute collagen was normalized to DNA (Figure 4.9.B).

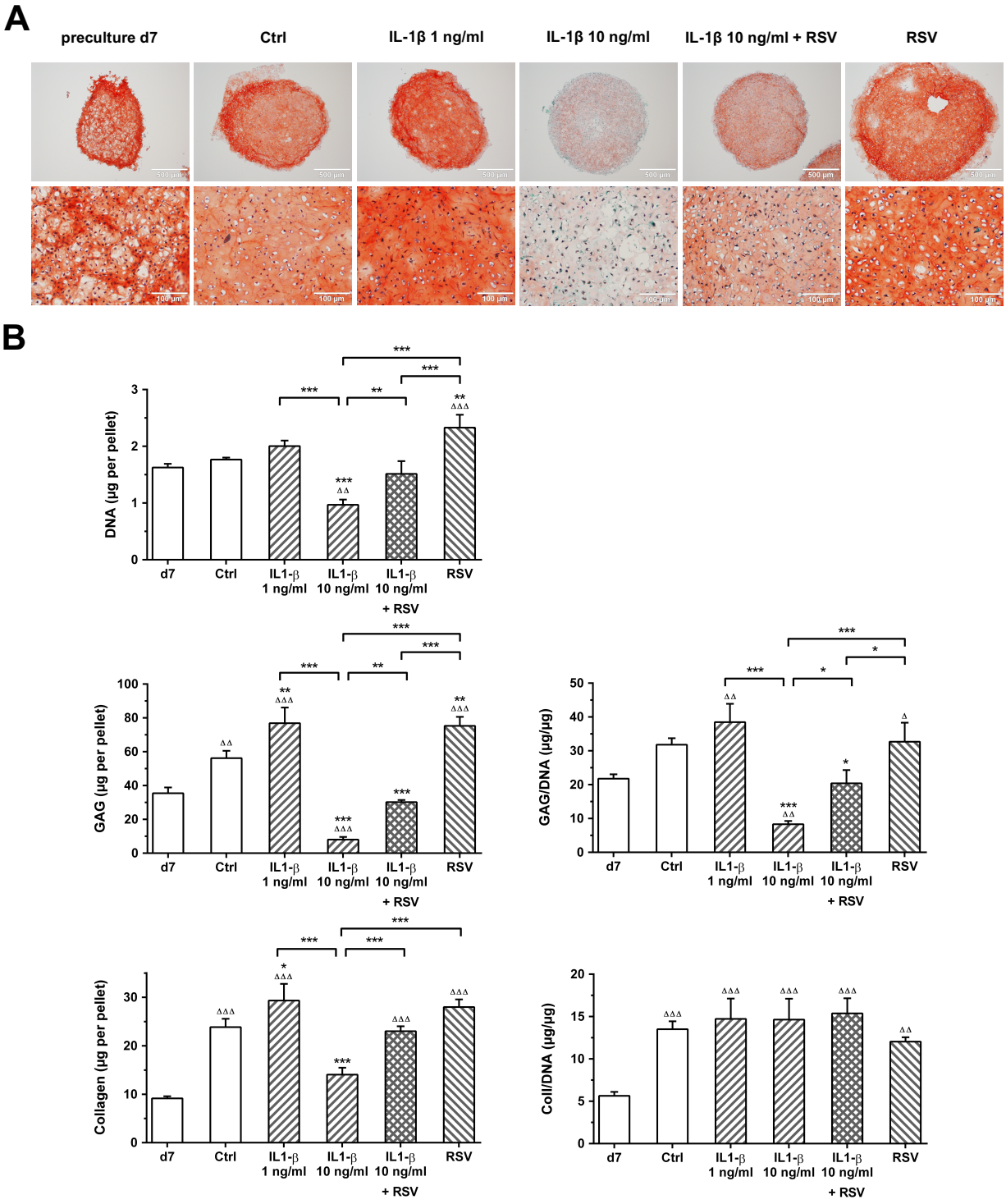

Figure 4.9. Construct analysis after 21 days of culture (7 days of precultivation in seeding medium containing FBS, followed by 14 days with different treatments): histological staining for GAG and quantitative biochemical assays. Data after 21 days is shown for all groups and compared to values at day 7. (**A**) Histological staining for GAG deposition with safranin-O. Scale bars represent 500 μm (upper) and 100 μm (lower). (**B**) DNA content per pellet, glycosaminoglycan (GAG) and collagen deposition of chondrocytes, shown for absolute amounts and normalized to DNA. Data are presented as means ± standard deviation (3 pellets per sample were pooled, with n=3). Asterisks above single bars represent statistical significance against control group after 21 days, above brackets between displayed groups; ***p<0.001, **p<0.01, *p<0.05. Triangles above single bars represent statistical significance between the respective treatment group after 21 days and control values at day 7; $^{\Delta\Delta\Delta}$p<0.001, $^{\Delta\Delta}$p<0.01, $^{\Delta}$p<0.05.

4.6.2 Preculture with RSV

In another set of experiments pellet constructs were initially precultured in chondrocyte medium supplemented with RSV (50 μM) for 7 days prior to culture with treatments for 14 days in order to evaluate the impact of RSV on subsequent culture in an inflammatory milieu (Figure 4.10).

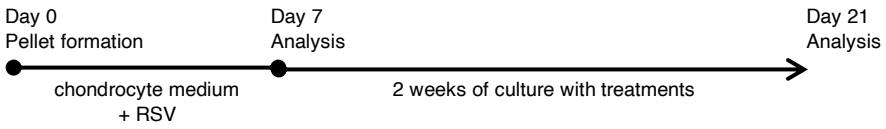

Figure 4.10. Preculture with RSV: Pellets were initially matured for 7 days before cultivation with treatments for 14 days. Within the preculture period they received chondrocyte medium supplemented with RSV (50 μM).

In terms of preculture with RSV (50 μM), subsequent culture in a highly inflammatory environment (IL-1β at 10 ng/ml) likewise led to a significantly lower DNA content, as compared to baseline levels at day 7 (IL-1β: 1.54±0.04 µg, day 7: 2.02±0.12 µg DNA; $p<0.05$) (Figure 4.11.B), whereas treatment with IL-1β at a concentration of only 1 ng/ml showed no significant difference in DNA content as compared to controls. Again, RSV counteracted the IL-1β-induced reduction of absolute DNA amount in a highly inflammatory milieu (IL-1β at 10 ng/ml) even up to control levels (Ctrl: 2.56±0.31 µg, IL-1β+RSV: 2.54±0.15 µg DNA) (Figure 4.11.B).

With regard to GAG deposition, treatment with IL-1β at 1 ng/ml once more resulted in a slightly but significantly higher GAG/DNA ratio as compared to controls (Ctrl: 39.94±4.24 µg/µg, IL-1β: 50.14±0.73 µg/µg GAG/DNA; $p<0.05$) and this was likewise supported by histological analysis (Figure 4.11.A). Still,

treatment with IL-1β at 10 ng/ml again drastically compromised GAG/DNA as compared to controls (IL-1β: 14.89±2.93 µg/µg, Ctrl: 39.94±4.24 µg/µg GAG/DNA; $p<0.001$), and values were once more significantly lower than baseline level at day 7 (day 7: 29.80±2.40 µg/µg GAG/DNA; $p<0.001$) (Figure 4.11.B). Co-treatment with RSV resulted in a reduced decrease of GAG content, when normalized to DNA even close to control levels (IL-1β+RSV: 32.38±4.24 µg/µg GAG/DNA) (Figure 4.11.B).

Concerning absolute collagen, a similar pattern as observed for GAG was ascertained. Apart from pellets receiving a highly inflammatory stimulus (IL-1β at 10 ng/ml) constructs in every other group exceeded day 7 values in terms of total collagen content. Constructs receiving both IL-1β (10 ng/ml) and RSV exhibited a significantly higher total collagen content than pellets cultured with IL-1β (10 ng/ml) only (IL-1β: 29.53±1.13 µg, IL-1β+RSV: 48.47±8.96 µg collagen; $p<0.01$). Yet, there was no significant difference between any treatment groups when absolute collagen was normalized to DNA (Figure 4.11.B).

When directly comparing the two different preculture regimes, precultivation with RSV (50 μM) led to an overall higher amount of total GAG and GAG/DNA, as well as especially a higher total collagen content as compared to precultivation in seeding medium containing FBS (10%). However, interestingly, precultivation with RSV (50 μM) resulted in a distinct enlargement of single cells, a morphological appearance associated with hypertrophy (Figure 4.11.A).

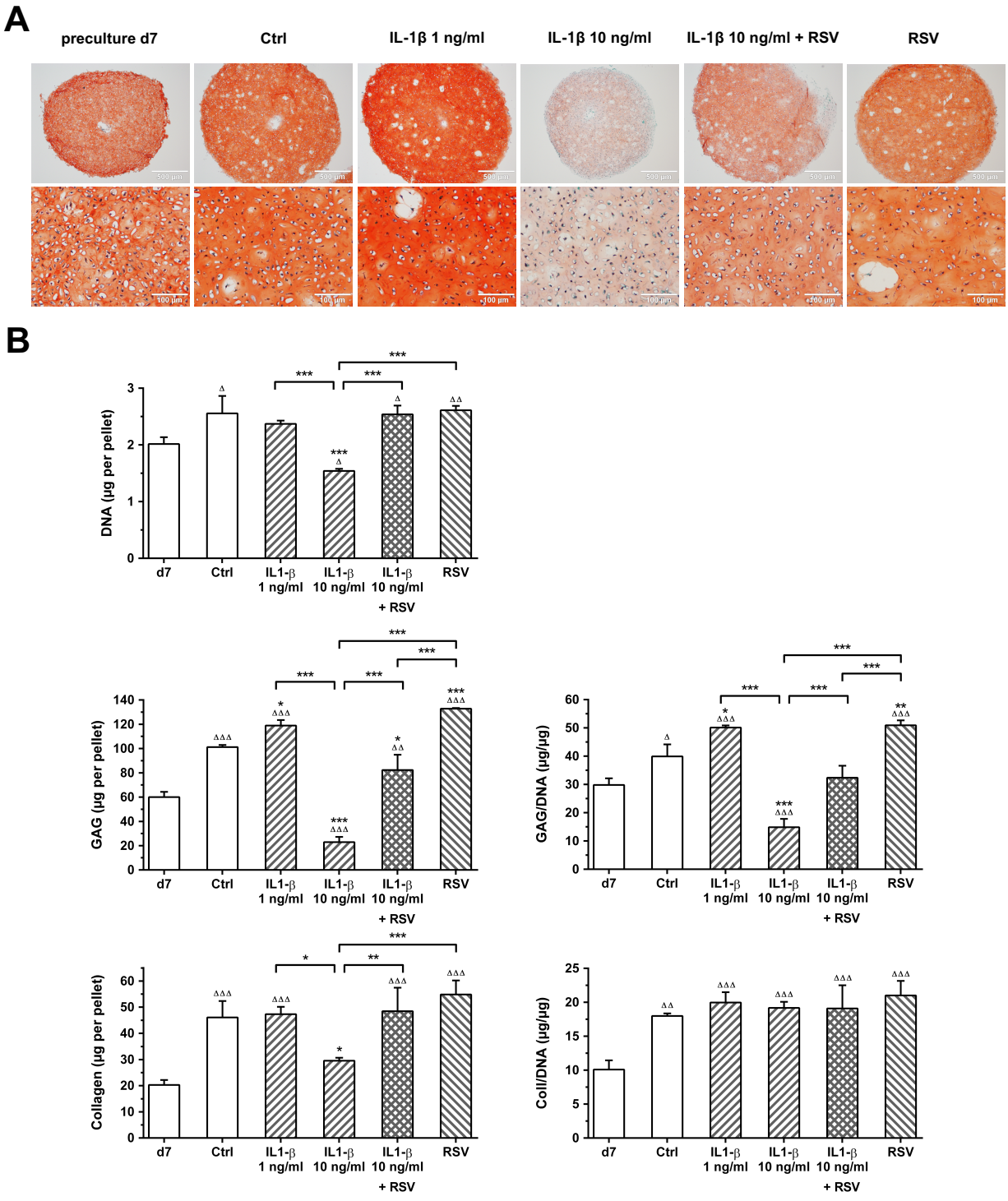

Figure 4.11. Construct analysis after 21 days of culture (7 days of precultivation in chondrocyte medium supplemented with RSV, followed by 14 days with different treatments): histological staining for GAG and quantitative biochemical assays. Data after 21 days is shown for all groups and compared to values at day 7. (**A**) Histological staining for GAG deposition with safranin-O. Scale bars represent 500 μm (upper) and 100 μm (lower). (**B**) DNA content per pellet, glycosaminoglycan (GAG) and collagen deposition of chondrocytes, shown for absolute amounts and normalized to DNA. Data are presented as means ± standard deviation (3 pellets per sample were pooled, with n=3). Asterisks above single bars represent statistical significance against control group after 21 days, above brackets between displayed groups; ***p<0.001, **p<0.01, *p<0.05. Triangles above single bars represent statistical significance between the respective treatment group after 21 days and control values at day 7; $^{\Delta\Delta\Delta}$p<0.001, $^{\Delta\Delta}$p<0.01, $^{\Delta}$p<0.05.

Part IV

Discussion

Chapter 5

Discussion

When striving for cell-based therapies in OA, pro-inflammatory conditions mediated by cytokines such as IL-1β need to be taken into account. In recent studies, RSV has exhibited potent anti-inflammatory properties (Shen *et al.*, 2012). However, long-term effects on 3D cartilaginous constructs under inflammatory conditions with regard to tissue quality, especially ECM composition, have remained unexplored.

Therefore, in the present study, long-term model cultures for cell-based therapies in an *in vitro* inflammatory environment were employed. Based on this, effects of RSV on the ECM content and the general appearance of 3D cartilaginous constructs in an IL-1β-induced inflammatory environment were examined. Thereby, special emphasis was set on ECM analyses and long-term construct development regarding cell-based therapies under inflammatory conditions.

This study is the first to demonstrate how RSV in a long-term *in vitro* culture potently affects ECM composition of 3D cartilaginous constructs in an inflammatory milieu.

5.1 Experimental design and choice of cell source

In order to simulate an inflammatory environment, IL-1β doses ranging from 1 to 10 ng/ml were used to ensure comparability with other *in vitro* studies in the literature (Djouad *et al.*, 2009; Im *et al.*, 2012; Schulze-Tanzil *et al.*, 2004). Regarding RSV, doses known from the literature with beneficial anti-inflammatory effects (Csaki *et al.*, 2009; Liu *et al.*, 2010; Maepa *et al.*, 2016) were tested in the employed experimental set-up to confirm that RSV in the applied dose was not detrimental to construct quality. Based on these results RSV was applied at 50 μM in the following experiments. Constructs were either treated with IL-1β (1 - 10 ng/ml), a combination of both inflammatory IL-1β and RSV as an anti-inflammatory stimulus, or RSV only in order to assess effects on pellets under non-inflammatory conditions. Pellets treated with chondrocyte medium only served as control. In one set of experiments pellets received treatments immediately for 14 days, whereas, in contrast, pellets in a second set were initially matured for 7 days before cultivation with treatments for 14 days. Indeed, precultured cartilage constructs have been shown to be less sensitive to cytokine treatment (Djouad *et al.*, 2009).

Pellet cultures are a well-established, standardized model specifically enabling investigations into ECM development. In *in vitro* studies like the present, isolated cells are used under controlled conditions, i.e., excluding factors such as stimulation by uncharacterized growth factors in the synovia, uncontrolled mechanical loading, and surrounding extracellular matrix components. Thus, in the present study an *in vitro* approach with isolated cells, which were additionally washed with PBS several times, was utilized.

An animal cell source, as utilized in the present study, bears benefits such as wide availability. Hence, a total of 340 porcine articular cartilage constructs were prepared for the experiments presented, without counting further preliminary

experiments. As first passage (P1) chondrocytes were utilized in order to work with differentiated rather than dedifferentiated cells, a large amount of primary porcine chondrocytes was isolated from approximately 30 femorotibial joints. Besides availability benefits, porcine and human articular chondrocytes share similarities (Schulze-Tanzil *et al.*, 2009). Indeed, porcine chondrocytes have been and are still employed in a large number of *in vitro* studies in the field (Bonitz *et al.*, 2019; Lin *et al.*, 2019; Vinardell *et al.*, 2012; Yin *et al.*, 2018).

5.2 Analyses of tissue quality and ECM composition

A strength of the experimental design employing pellet constructs is the capability to precisely monitor ECM development. Specific focus was set on ECM composition including GAG and collagen content. Whereas it has already been shown that RSV exhibits anabolic and anti-inflammatory potential (Shen *et al.*, 2012, Im *et al.*, 2012), besides mere accumulation of GAG content, the differentiation of ECM components is of major interest concerning cell-based therapies. Within the present study, GAG content was determined by histology and biochemical quantification for ECM analyses. Thereby, both total GAG and GAG per DNA ratio, representing matrix composition normalized to DNA, were considered. Concerning collagen expression, total content was measured using biochemical quantification methods. Besides that, both IHC, reflecting protein expression, and qRT-PCR, reflecting current gene expression, were utilized to examine specific types of collagen.

5.3 IL-1β exhibits catabolic impact on chondrocytes and ECM

The inflammatory cytokine IL-1β was applied in doses ranging from 1-10 ng/ml in order to ensure comparability with other *in vitro* studies in the literature (Djouad *et al.*, 2009; Im *et al.*, 2012; Schulze-Tanzil *et al.*, 2004). Even though some studies analyzing tissue from OA patients found lower concentrations of inflammatory mediators in the synovial fluid (Sohn *et al.*, 2012), establishing effective doses especially within an experimental *in vitro* set-up requires consideration of shorter exposure to the stimulus as effects are determined by dose and time. Within the present study, a dose-dependent catabolic impact by IL-1β on both cell number and ECM content was observed. While IL-1β at 1 ng/ml hardly exhibited any effects on the chondrocyte pellets, IL-1β at 10 ng/ml caused drastic alterations in terms of reduced construct diameter and DNA content, and strongly altered ECM composition. These IL-1β-treated constructs revealed a distinct expression of the cartilage-degrading enzyme MMP13, were almost depleted of GAG, had a decreased total collagen content, and displayed marked expression of collagen type I, a marker for fibrous cartilage. Even though IHC signal for collagen type II appeared to be more intense in IL-1β (10 ng/ml) treated samples, quantitative biochemical assays revealed low absolute collagen content on a total scale as well as normalized to DNA.

5.4 RSV as attractive adjuvant treatment in cell-based therapies

Regarding repair and tissue engineering techniques for articular cartilage in inflammatory OA, there is emerging progress suggesting that anti-inflammatory drugs, by exhibiting beneficial effects at the defect site, may delay advancement

of deterioration (Djouad *et al.*, 2009; Makris *et al.*, 2015). In previous short-term studies, which were mainly carried out in chondrocyte monolayer culture, increasing evidence has been revealed that RSV can counteract inflammatory signaling, with several pathways being under consideration (Shen *et al.*, 2012). RSV has been found to induce anti-apoptotic effects by suppressing IL-1β-mediated activation of caspase-3 and the cleavage of the DNA repair enzyme poly(ADP-ribose)polymerase (PARP) (Csaki *et al.*, 2008; Shakibaei *et al.*, 2007). In the same context, RSV has been reported to counteract IL-1β-mediated production of PGE_2 and COX-2 activity in chondrocytes when co-treated for 24 hours (Dave *et al.*, 2008). Moreover, RSV inhibited IL-1β-mediated nuclear translocation of NF-κB as well as NF-κB-regulated gene products participating in inflammation (VEGF, COX-2, MMP-3, MMP-9) in human articular chondrocytes in investigations for up to 48 hours (Csaki *et al.*, 2009; Shakibaei *et al.*, 2008). Thus, RSV appears as an attractive adjuvant treatment, which may potentially enable cell-based therapeutic approaches in OA.

Nonetheless, *in vitro* experiments so far have primarily focused on the elucidation of signaling pathways in short-term settings, and data in a 3D culture model is rare. Thus, in this study the effects of RSV were investigated in model cultures for cell-based therapeutic approaches in an OA milieu, applying pellets made from expanded articular chondrocytes in an IL-1β-mediated inflammatory environment. For the first time, distinct effects of RSV on the ECM composition of 3D cartilaginous constructs in a long-term *in vitro* culture are demonstrated.

5.5 RSV attenuates catabolic effects induced by IL-1β

In the present study, it was investigated if RSV, in a 14-days long-term culture set-up, affected the general appearance and ECM content of 3D cartilaginous constructs under inflammatory conditions (IL-1β, 10 ng/ml). RSV was employed at 50 μM, a concentration that has previously been demonstrated to effectively induce expression of collagen type II and attenuate IL-1β-mediated apoptosis in articular chondrocytes (Csaki *et al.*, 2009; Liu *et al.*, 2010; Maepa *et al.*, 2016).

Treatment with RSV in an inflammatory setting indeed counteracted the drastic catabolic impact observed when constructs were cultured with IL-1β only. In that context, IL-1β (10 ng/ml) significantly depleted GAG content as well as collagen content both on absolute scale and normalized to DNA, and, besides this effect on ECM deposition, strongly diminished total DNA content and absolute diameter of the treated constructs. RSV inhibited the strong reduction in pellet diameter and DNA amount, and the distinct upregulation of MMP13 expression triggered by IL-1β was counteracted by RSV. As compared to treatment with IL-1β alone, co-treatment with RSV vastly increased absolute GAG content and GAG/DNA. Moreover, total collagen content was enhanced as well, whereas immunohistochemical staining for adverse collagen type I was markedly enhanced by IL-1β and still identified upon co-treatment with RSV.

The considerably strong counteraction of IL-1β-mediated catabolic effects by RSV was accordant with protein expression studies for up to 48 hours showing that RSV reduced IL-1β-mediated down-regulation of collagen type II and aggrecan in monolayer culture (Liu *et al.*, 2010; Shakibaei *et al.*, 2007) and also chitosan-gelatin scaffolds (Lei *et al.*, 2008). Furthermore, RSV has previously been demonstrated to partly inhibit mRNA expression of MMP1, MMP3, MMP13, and collagen type I in chondrocytes under inflammatory conditions mediated by LPS in a hydrogel composed of hyaluronic acid/resveratrol (Sheu *et*

al., 2013). Moreover, it was recently reported that RSV integrated in a cell-free PLA-gelatin porous nano-scaffold supported repair in a posttraumatic cartilage defect model in rats, with an increased collagen type II expression and decreased MMP13 expression (Yu *et al.*, 2018).

5.6 RSV counteracts IL-1β-mediated impairment of ECM deposition independently from preculture set-up

In an additional approach within the current study, constructs were precultured for 7 days before exposing them to the IL-1β-induced inflammatory milieu for another 14 days. Within the preculture period they either received chondrocyte medium only, seeding medium containing FBS (10%) or chondrocyte medium supplemented with RSV (50 μM) (Figure 3.1). Previously, precultured cartilage constructs have been shown to be less sensitive to cytokine treatment (Djouad *et al.*, 2009). Within the present study, in comparison of both control groups (i.e. 'w/o preculture' and 'with preculture' in only chondrocyte medium), experiments with preculture exhibited a higher GAG content due to maturation. However, loss of DNA amount and decrease of ECM components upon treatment with IL-1β was not prevented by preculture. Generally, data from this experimental set-up confirmed RSV as an effective treatment inhibiting the deleterious effects of the inflammatory cytokine. As compared to constructs after only 7 days of preculture, IL-1β (10 mg/ml) led to markedly decreased absolute GAG content and GAG/DNA, indicating ECM degradation. RSV counteracted depletion in an inflammatory environment and led to a pronounced rescue of GAG content, which was, interestingly, even more distinct (up to control levels) in pellets obtaining initial maturation compared to those without preculture.

These results further emphasized the relevance of specifically assessing the point in time when exposing chondrocyte constructs to a pathophysiological environment. Similar results were obtained when pellets were precultured with FBS (10 %) and RSV (50 μM), respectively (Figure 4.9, Figure 4.11). These additional experiments were carried out to investigate whether in preculture applied agents potentially influence construct quality. Consistent with the preculture experiment in only chondrocyte medium, RSV exhibited potent anti-inflammatory properties. These observations emphasize the robustness of the finding that RSV counteracts the IL-1β-mediated impairment of ECM deposition in 3D articular chondrocyte constructs. Interestingly, preculture with RSV resulted in a more pronounced rescue of DNA, GAG, and collagen content.

5.7 RSV induces collagen type X induction under non-inflammatory conditions

RSV was investigated under non-inflammatory conditions as a further control group in both experimental set-ups, i.e., without and with preculture. In accordance with findings published by Im *et al.* (Im *et al.*, 2012) that RSV alone increased GAG accumulation per cell in a long-term *in vitro* culture, RSV within the present study enhanced absolute GAG content and GAG/DNA. Furthermore, in the set-up with preculture, collagen type II gene expression was enhanced by RSV, which also affirmed previous data obtained by Maepa *et al.* in monolayer cultures of porcine articular chondrocytes (Maepa *et al.*, 2016). Moreover, RSV induced gene expression and protein accumulation of collagen type X, a marker for hypertrophy, under non-inflammatory conditions in articular chondrocyte constructs, which was consistent with results found by

Kim *et al.* in monolayer and 3D cultures (Kim *et al.*, 2014). As formation of hypertrophic cells is rather to be avoided, this finding may potentially be critical for the application of RSV in cell-based therapy. Yet, a lower RSV dose may conceivably be related to prevention of such side effects. Interestingly, under the culture set-ups receiving inflammatory stimuli in the present study, RSV (at 50 μM) mitigated IL-1β-induced effects (at 10 ng/ml), but did not cause collagen type X accumulation, which was further in accordance with qRT-PCR analysis.

5.8 Limitations of the study and future plans

In the present study, to further gain insight into the gene expression of cultured chondrocytes, qRT-PCR analyses were performed. As they were conducted at day 14 for experiments without preculture and day 21 for experiments with preculture, respectively, gene expression results may not be representative for expression levels during the entire culture period.

Also, concerning correlation of total DNA content with number of viable cells, supporting viability data such as live-dead staining (as described previously by Böck *et al.*, 2018) at different points of time might be of interest.

Based on the literature (Csaki *et al.*, 2009; Liu *et al.*, 2010; Maepa *et al.*, 2016) RSV was applied at 50 μM, a dose which induced collagen type X expression under non-inflammatory conditions. Regarding potential hypertrophic effects of RSV in a non-inflammatory environment, further *in vitro* experiments examining multiple concentrations of RSV appear desirable. Also, subsequent studies may further consider constructs at different periods of development exposed to inflammatory conditions utilizing a potential adjuvant treatment such as RSV. Based on the results in this study, further research regarding impact of RSV

under various inflammatory conditions (including IL-1β at 1 ng/ml) appears desirable concerning potential therapeutic applicability.

5.9 Conclusion and potential application of RSV as future clinical therapeutic

Taken together, the present study found RSV to elicit marked beneficial effects on the ECM composition of 3D cartilaginous constructs in long-term inflammatory culture *in vitro*. RSV treatment counteracted IL-1β-mediated ECM degradation and resulted in partial rescue of cartilaginous matrix deposition, especially GAG, affected by IL-1β. Upon preculture, rescue of GAG and collagen content by RSV was even enhanced up to control levels. RSV in a non-inflammatory environment likewise enhanced GAG synthesis, but also upregulated collagen type X expression.

Even though RSV has been demonstrated to exhibit potent anti-inflammatory properties, its eventual clinical use for OA patients should further be investigated. Regarding RSV pharmacokinetics (Walle, 2011), there has been some recent progress to improve oral bioavailability, including encapsulation of RSV in various dosage forms, such as polymeric particles, liposomes, lipid nanocarriers, micelles, nanoemulsions, and others (Chimento *et al.*, 2019). Currently, a phase III clinical trial for oral resveratrol in knee osteoarthritis (ARTHROL) is ongoing. This study is following the published protocol for a multicenter randomized double-blind placebo-controlled trial (Nguyen *et al.*, 2017). Apart from that, as a further form of application, Yu *et al.* have characterized a non-seeded PLA-gelatin porous nano-scaffold with incorporated RSV molecules (Yu *et al.*, 2018). Another potential translation to clinical

applicability might be through intra-articular injection of RSV, as local intra-articular injection of RSV delayed cartilage degeneration in OA mice (Qin *et al.*, 2017).

Future studies should, nevertheless, also explicitly take potential hypertrophic effects into account before RSV may be considered as a co-treatment when exposing chondrocyte constructs to an inflammatory environment such as predominant in OA.

Part V

Summary

Chapter 6

Summary

Articular cartilage is an exceptional connective tissue which by a network of fibrillar collagen and glycosaminoglycan (GAG) molecules allows both low-friction articulation and distribution of loads to the subchondral bone (Armiento et al., 2018, Ulrich-Vinther et al., 2003). Because of its very limited ability to self-repair, chondral defects following traumatic injury increase the risk for secondary osteoarthritis (OA) (Muthuri et al., 2011). Still, current OA treatments such as common nonsteroidal anti-inflammatory drugs (NSAIDs) and joint replacement primarily address end-stage symptoms (Tonge et al., 2014). As low-grade inflammation plays a pivotal role in the pathogenesis of OA (Robinson et al., 2016), there is a strong demand for novel therapeutic concepts, such as integrating application of anti-inflammatory agents into cartilage cell-based therapies in order to effectively treat OA affected joints in early disease stages. The polyphenolic phytoalexin resveratrol (RSV), found in the skin of red grapes, berries, and peanuts, has been shown to have effective anti-inflammatory properties (Shen et al., 2012). However, its long-term effects on 3D chondrocyte constructs cultured in an inflammatory environment with regard to tissue quality have remained unexplored so far. Therefore, in this study, pellets made from expanded porcine articular chondrocytes were cultured for 14 days with either the pro-inflammatory cytokine interleukin-1β (IL-1β) (1 - 10 ng/ml) or RSV (50 μM) alone, or a co-treatment with both agents. Constructs treated with chondrocyte medium only served as control. Treatment with IL-1β at 10 ng/ml resulted in a significantly smaller pellet size and reduced DNA content.

However, RSV counteracted the IL-1β-induced decrease and significantly enhanced diameter and DNA content. Also, in terms of GAG deposition, treatment with IL-1β at 10 ng/ml resulted in a tremendous depletion of absolute GAG content and GAG/DNA. Again, RSV co-treatment counteracted the inflammatory stimulus and led to a partial recovery of GAG content. Histological analysis utilizing safranin-O staining confirmed these findings. Marked expression of the cartilage-degrading enzyme matrix metalloproteinase 13 (MMP13) was detected in IL-1β-treated pellets, but none upon RSV co-treatment. Moreover, co-treatment of IL-1β-challenged constructs with RSV significantly increased absolute collagen content. However, under non-inflammatory conditions, RSV induced gene expression and protein accumulation of collagen type X, a marker for undesirable hypertrophy. Taken together, in the present thesis, RSV was demonstrated to elicit marked beneficial effects on the extracellular matrix composition of 3D cartilaginous constructs in long-term inflammatory culture in vitro, but also induced hypertrophy under non-inflammatory conditions. Based on these findings, further experiments examining multiple concentrations of RSV under various inflammatory conditions appear desirable concerning potential therapeutic applicability in OA.

Chapter 7

Zusammenfassung

Gelenkknorpel ermöglicht als spezielles Bindegewebe aus Kollagenfasern und Glykosaminoglykanen (GAG) sowohl die reibungsarme Beweglichkeit in Gelenken als auch die Lastübertragung auf angrenzende Knochen (Armiento et al., 2018, Ulrich-Vinther et al., 2003). Aufgrund der sehr begrenzten Fähigkeit zur intrinsischen Erneuerung erhöhen chondrale Defekte nach traumatischen Verletzungen das Risiko für sekundäre Arthrose (Osteoarthritis; OA) (Muthuri et al., 2011). Dennoch konzentrieren sich derzeitige Behandlungsansätze, einschließlich nichtsteroidaler Antirheumatika (NSAR) und des operativen Gelenkersatzes, hauptsächlich auf Symptome im Endstadium der Erkrankung (Tonge et al., 2014). Da eine geringgradige Entzündung eine entscheidende Rolle in der Pathogenese der Arthrose spielt (Robinson et al., 2016), besteht ein starker Bedarf an neuartigen Therapiekonzepten, wie der Kombination von anti-inflammatorischen Wirkstoffen mit knorpelzellbasierten Therapien, um von Arthrose betroffene Gelenke in frühen Krankheitsstadien wirksam zu behandeln. Das polyphenolische Phytoalexin Resveratrol (RSV), welches in der Schale roter Weintrauben, in Beeren und Erdnüssen vorkommt, besitzt starke entzündungshemmende Eigenschaften (Shen et al., 2012). Langzeiteffekte auf 3D-Knorpelkonstrukte unter inflammatorischen Bedingungen sind hinsichtlich der Gewebequalität jedoch bislang unerforscht geblieben. Daher wurden in der vorliegenden Studie Pellets aus expandierten porcinen Gelenkknorpelzellen über einen Zeitraum von 14 Tagen entweder mit dem pro-inflammatorischen Zytokin Interleukin-1β (IL-1β) (1 - 10 ng/ml) oder RSV (50 μM) allein, oder mit beiden

Agenzien kombiniert behandelt. Konstrukte, welche nur serumfreies Chondrozytenmedium erhielten, dienten als Kontrolle. Die Behandlung mit IL-1β in einer Konzentration von 10 ng/ml führte zu einem signifikant geringeren Durchmesser der Pellets sowie einem verringerten DNA-Gehalt. RSV wirkte dieser IL-1β-vermittelten Reduktion entgegen und steigerte signifikant sowohl Durchmesser als auch DNA-Gehalt der untersuchten Konstrukte. Auch in Bezug auf die Deposition von GAG-Molekülen führte die Kultur mit IL-1β (10 ng/ml) zu einer massiven Abnahme des absoluten GAG-Gehaltes und der GAG/DNA-Ratio. Abermals wirkte die gleichzeitige Behandlung mit RSV dem Entzündungsreiz deutlich entgegen und resultierte in einer partiellen Wiederherstellung des GAG-Gehaltes. Die histologische Analyse unter Verwendung von Safranin-O-Färbungen bestätigte diese Ergebnisse. Darüber hinaus manifestierte sich eine ausgeprägte Expression des knorpelabbauenden Enzyms Matrix-Metalloproteinase 13 (MMP13) in IL-1β behandelten Pellets, nicht jedoch in denen, die simultan mit RSV behandelt wurden. Außerdem resultierte die gleichzeitige Behandlung von IL-1β-stimulierten Konstrukten mit RSV in einer signifikanten Erhöhung des absoluten Kollagengehaltes. Unter nicht-inflammatorischen Bedingungen induzierte RSV die Genexpression und Proteinakkumulation von Kollagen Typ X, einem Marker für unerwünschte Hypertrophie. Zusammengefasst wurde in der vorliegenden Arbeit gezeigt, dass RSV deutliche positive Effekte auf die Extrazellulärmatrix von 3D-Knorpelkonstrukten in einer Langzeit-Entzündungskultur in vitro hervorruft, allerdings unter nicht-inflammatorischen Bedingungen Hypertrophie induziert. Basierend auf diesen Befunden erscheinen weitere Experimente zur Untersuchung unterschiedlicher RSV-Konzentrationen unter verschiedenen Entzündungsbedingungen hinsichtlich einer möglichen therapeutischen Anwendbarkeit bei OA wünschenswert.

Part VI

References

References

Adkisson, H. D., Martin, J. A., Amendola, R. L., Milliman, C., Mauch, K. A., Katwal, A. B., Seyedin, M., Amendola, A., Streeter, P. R., & Buckwalter, J. A. (2010). The potential of human allogeneic juvenile chondrocytes for restoration of articular cartilage. The American Journal of Sports Medicine, 38, 1324–1333. doi:10.1177/0363546510361950

Altman, R., Alarcón, G., Appelrouth, D., Bloch, D., Borenstein, D., Brandt, K., Brown, C., Cooke, T. D., Daniel, W., Feldman, D., Greenwald, R., Hochberg, M., Howell, D., Ike, R., Kapila, P., Kaplan, D., Koopman, W., Marino, C., McDonald, E., . . . Wolfe, F. (1991). The American College of Rheumatology criteria for the classification and reporting of osteoarthritis of the hip. Arthritis & Rheumatism, 34, 505–514. doi:10.1002/art.1780340502

Anderson, D. E., & Johnstone, B. (2017). Dynamic mechanical compression of chondrocytes for tissue engineering: a critical review. Frontiers in Bioengineering and Biotechnology, 5, 76. doi:10.3389/fbioe.2017.00076

Armiento, A. R., Alini, M., & Stoddart, M. J. (2019). Articular fibrocartilage - Why does hyaline cartilage fail to repair? Advanced Drug Delivery Reviews, 146, 289-305. doi:10.1016/j.addr.2018.12.015

Armiento, A. R., Stoddart, M. J., Alini, M., & Eglin, D. (2018). Biomaterials for articular cartilage tissue engineering: learning from biology. Acta Biomaterialia, 65, 1-20. doi:10.1016/j.actbio.2017.11.021

Aydelotte, M. B., Greenhill, R. R., & Kuettner, K. E. (1988). Differences between sub-populations of cultured bovine articular chondrocytes. II. Proteoglycan metabolism. Connective Tissue Research, 18, 223-234. doi:10.3109/03008208809016809

Blagojevic, M., Jinks, C., Jeffery, A., & Jordan, K. P. (2010). Risk factors for onset of osteoarthritis of the knee in older adults: a systematic review and meta-analysis. Osteoarthritis and Cartilage, 18, 24-33. doi:10.1016/j.joca.2009.08.010

Blunk, T., Sieminski, A. L., Gooch, K. J., Courter, D. L., Hollander, A. P., Nahir, A. M., Langer, R., Vunjak-Novakovic, G., & Freed, L. E. (2002). Differential effects of growth factors on tissue-engineered cartilage. Tissue Engineering, 8, 73-84. doi:10.1089/107632702753503072

Böck, T., Schill, V., Krähnke, M., Steinert, A. F., Tessmar, J., Blunk, T., & Groll, J. (2018). TGF-β1-modified hyaluronic acid/poly(glycidol) hydrogels for chondrogenic differentiation of human mesenchymal stromal cells. Macromolecular Bioscience, 18, 1700390. doi:10.1002/mabi.201700390

Bonitz, M., Schaffer, C., Amling, M., Poertner, R., Schinke, T., & Jeschke, A. (2019). Secreted factors from synovial fibroblasts immediately regulate gene expression in articular chondrocytes. Gene, 698, 1-8. doi:10.1016/j.gene.2019.02.065

Carballo, C. B., Nakagawa, Y., Sekiya, I., & Rodeo, S. A. (2017). Basic science of articular cartilage. Clinics in Sports Medicine, 36, 413-425. doi:10.1016/j.csm.2017.02.001

Cerejo, R., Dunlop, D. D., Cahue, S., Channin, D., Song, J., & Sharma, L. (2002). The influence of alignment on risk of knee osteoarthritis progression according to baseline stage of disease. Arthritis & Rheumatism, 46, 2632–2636. doi:10.1002/art.10530

Chimento, A., De Amicis, F., Sirianni, R., Sinicropi, M. S., Puoci, F., Casaburi, I., Saturnino, C., & Pezzi, V. (2019). Progress to improve oral bioavailability and beneficial effects of resveratrol. International Journal of Molecular Sciences, 20, E1381. doi:10.3390/ijms20061381

Chowdhury, T. T., Salter, D. M., Bader, D. L., & Lee, D. A. (2008). Signal transduction pathways involving p38 MAPK, JNK, NFkappaB and AP-1 influences the response of chondrocytes cultured in agarose constructs to IL-1beta and dynamic compression. Inflammation Research, 57, 306-313. doi:10.1007/s00011-007-7126-y

Cohen, S. B., Proudman, S., Kivitz, A. J., Burch, F. X., Donohue, J. P., Burstein, D., Sun, Y. N., Banfield, C., Vincent, M. S., Ni, L., & Zack, D. J. (2011). A randomized, double-blind study of AMG 108 (a fully human monoclonal antibody to IL-1R1) in patients with osteoarthritis of the knee. Arthritis Research & Therapy, 13, R125. doi:10.1186/ar3430

Crawford, D. C., DeBerardino, T. M., & Williams, R. J. (2012). NeoCart, an autologous cartilage tissue implant, compared with microfracture for treatment of distal femoral cartilage lesions: an FDA phase-II prospective, randomized clinical trial after two years. The Journal of Bone & Joint Surgery, 94, 979–989. doi:10.2106/JBJS.K.00533

Croft, P., Coggon, D., Cruddas, M., & Cooper, C. (1992). Osteoarthritis of the hip: an occupational disease in farmers. BMJ, 304, 1269–1272. doi:10.1136/bmj.304.6837.1269

Csaki, C., Keshishzadeh, N., Fischer, K., & Shakibaei, M. (2008). Regulation of inflammation signalling by resveratrol in human chondrocytes in vitro. Biochemical Pharmacology, 75, 677-687. doi:10.1016/j.bcp.2007.09.014

Csaki, C., Mobasheri, A., & Shakibaei, M. (2009). Synergistic chondroprotective effects of curcumin and resveratrol in human articular chondrocytes: inhibition of IL-1beta-induced NF-kappaB-mediated inflammation and apoptosis. Arthritis Research & Therapy, 11, R165. doi:10.1186/ar2850

Culav, E. M., Clark, C. H., & Merrilees, M. J. (1999). Connective tissues: matrix composition and its relevance to physical therapy. Physical Therapy, 79, 308-319.

Dave, M., Attur, M., Palmer, G., Al-Mussawir, H. E., Kennish, L., Patel, J., & Abramson, S. B. (2008). The antioxidant resveratrol protects against chondrocyte apoptosis via effects on mitochondrial polarization and ATP production. Arthritis & Rheumatism, 58, 2786-2797. doi:10.1002/art.23799

Deng, Z., Li, Y., Liu, H., Xiao, S., Li, L., Tian, J., Cheng, C., Zhang, G., & Zhang, F. (2019). The role of sirtuin 1 and its activator, resveratrol in osteoarthritis. Bioscience Reports, 39, BSR20190189. doi:10.1042/BSR20190189

Djouad, F., Rackwitz, L., Song, Y., Janjanin, S., & Tuan, R. S. (2009). ERK1/2 activation induced by infammatory cytokines compromises effective host tissue integration of engineered cartilage. Tissue Engineering: Part A, 15, 2825-2835. doi: 10.1089/ten.tea.2008.0663

DuRaine, G. D., Brown, W. E., Hu, J. C., & Athanasiou, K. A. (2015). Emergence of scaffold-free approaches for tissue engineering musculoskeletal cartilages. Annals of Biomedical Engineering, 43, 543-554. doi:10.1007/s10439-014-1161-y

Endres, M., Andreas, K., Kalwitz, G., Freymann, U., Neumann, K., Ringe, J., Sittinger, M., Haupl, T., & Kaps, C. (2010). Chemokine profile of synovial fluid from normal, osteoarthritis and rheumatoid arthritis patients: CCL25, CXCL10 and XCL1 recruit human subchondral mesenchymal progenitor cells. Osteoarthritis and Cartilage, 18, 1458-1466. doi:10.1016/j.joca.2010.08.003

Eyre, D. R. (2004). Collagens and cartilage matrix homeostasis. Clinical Orthopaedics and Related Research, 427S, S118-S122. doi:10.1097/01.blo.0000144855.48640.b9

Farndale, R. W., Buttle, D. J., & Barrett, A. J. (1986). Improved quantitation and discrimination of sulphated glycosaminoglycans by use of dimethylmethylene blue. Biochimica et Biophysica Acta, 883, 173-177. doi:10.1016/0304-4165(86)90306-5

Felson, D. T., Lawrence, R. C., Dieppe, P. A., Hirsch, R., Helmick, C. G., Jordan, J. M., Kington, R. S., Lane, N. E., Nevitt, M. C., Zhang, Y., Sowers, M., McAlindon, T., Spector, T. D., Poole, A. R., Yanovski, S. Z., Ateshian, G., Sharma, L., Buckwalter, J. A., Brandt, K. D., & Fries, J. F. (2000). Osteoarthritis: new insights. Part 1: the disease and its risk factors. Annals of Internal Medicine, 133, 635-646. doi:10.7326/0003-4819-133-8-200010170-00016

Foell, D., Wittkowski, H., & Roth, J. (2007). Mechanisms of disease: a 'DAMP' view of inflammatory arthritis. Nature Clinical Practice Rheumatology, 3, 382-390. doi:10.1038/ncprheum0531

Gobezie, R., Kho, A., Krastins, B., Sarracino, D. A., Thornhill, T. S., Chase, M., Millett, P. J., & Lee, D. M. (2007). High abundance synovial fluid proteome: distinct profiles in health and osteoarthritis. Arthritis Research & Therapy, 9, R36. doi:10.1186/ar2172

Goldring, M. B., Fukuo, K., Birkhead, J. R., Dudek, E., & Sandell, L. J. (1994). Transcriptional suppression by interleukin-1 and interferon-γ of type II collagen gene expression in human chondrocytes. Journal of Cellular Biochemistry, 54, 85-99. doi:10.1002/jcb.240540110

Gredes, T. (2008). Investigation of gene expression in condylar cartilage of pigs (sus scrofa domesticus) following anterior mandibular displacement. Dissertation, Ernst-Moritz-Arndt-University, Greifswald, Germany.

Grotle, M., Hagen, K. B., Natvig, B., Dahl, F. A., & Kvien, T. K. (2008). Obesity and osteoarthritis in knee, hip and/or hand: an epidemiological study in the general population with 10 years follow-up. BMC Musculoskeletal Disorders, 9, 132. doi:10.1186/1471-2474-9-132

Guermazi, A., Roemer, F. W., Hayashi, D., Crema, M. D., Niu, J., Zhang, Y., Marra, M. D., Katur, A., Lynch, J. A., El-Khoury, G. Y., Baker, K., Hughes, L. B., Nevitt, M. C., & Felson, D. T. (2011). Assessment of synovitis with contrast-enhanced MRI using a whole-joint semiquantitative scoring system in people with, or at high risk of, knee osteoarthritis: the MOST study. Annals of the Rheumatic Diseases, 70, 805-811. doi:10.1136/ard.2010.139618

Hollander, A. P., Heathfield, T. F., Webber, C., Iwata, Y., Bourne, R., Rorabeck, C., & Poole, A. R. (1994). Increased damage to type II collagen in osteoarthritic articular cartilage detected by a new immunoassay. The Journal of Clinical Investigation., 93, 1722-1732. doi:10.1172/JCI117156

Huang, B. J., Hu, J. C., & Athanasiou, K. A. (2016). Cell-based tissue engineering strategies used in the clinical repair of articular cartilage. Biomaterials, 98, 1-22. doi:10.1016/j.biomaterials.2016.04.018

Im, H. J., Li, X., Chen, D., Yan, D., Kim, J., Ellman, M. B., Stein, G. S., Cole, B., Kc, R., Cs-Szabo, G., & van Wijnen, A. J. (2012). Biological effects of the plant-derived polyphenol resveratrol in human articular cartilage and chondrosarcoma cells. Journal of Cellular Physiology, 227, 3488-3497. doi:10.1002/jcp.24049

Jenei-Lanzl, Z., Meurer, A., & Zaucke, F. (2019). Interleukin-1β signaling in osteoarthritis - chondrocytes in focus. Cellular Signalling, 53, 212-223. doi:10.1016/j.cellsig.2018.10.005

Jiang, L., Tian, W., Wang, Y., Rong, J., Bao, C., Liu, Y., Zhao, Y., & Wang, C. (2012). Body mass index and susceptibility to knee osteoarthritis: a systematic review and meta-analysis. Joint Bone Spine, 79, 291–297. doi:10.1016/j.jbspin.2011.05.015

Johnson, V. L., & Hunter, D. J. (2014). The epidemiology of osteoarthritis. Best Practice & Research: Clinical Rheumatology, 28, 5–15. doi:10.1016/j.berh.2014.01.004

Johnstone, B., Alini, M., Cucchiarini, M., Dodge, G. R., Eglin, D., Guilak, F., Madry, H., Mata, A., Mauck, R. L., Semino, C. E., & Stoddart, M. J. (2013). Tissue engineering for articular cartilage repair - the state of the art. European Cells & Materials, 25, 248-267. doi:10.22203/ecm.v025a18

Kellgren, J. H., & Lawrence, J. S. (1957). Radiological assessment of osteo-arthrosis. Annals of the Rheumatic Diseases, 16, 494–502. doi:10.1136/ard.16.4.494

Kellner, K., Schulz, M. B., Göpferich, A., & Blunk, T. (2001). Insulin in tissue engineering of cartilage: a potential model system for growth factor application. Journal of Drug Targeting, 9, 439-448. doi:10.3109/10611860108998778

Kempson, G. E., Muir, H., Swanson, S. A., & Freeman, M. A. (1970). Correlations between stiffness and the chemical constituents of cartilage on the human femoral head. Biochimica et Biophysica Acta - General Subjects, 215, 70-77. doi:10.1016/0304-4165(70)90388-0

Kim, H. J., Braun, H. J., & Dragoo J. L. (2014). The effect of resveratrol on normal and osteoarthritic chondrocyte metabolism. Bone & Joint Research, 3, 51-59. doi:10.1302/2046-3758.33.2000226

Kim, Y. J., Sah, R. L., Doong, J. Y., & Grodzinsky, A. J. (1988). Fluorometric assay of DNA in cartilage explants using Hoechst 33258. Analytical Biochemistry, 174, 168-176. doi:10.1016/0003-2697(88)90532-5

Kon, E., Filardo, G., Berruto, M., Benazzo, F., Zanon, G., Della Villa, S., & Marcacci, M. (2011). Articular cartilage treatment in high-level male soccer players: a prospective comparative study of arthroscopic second-generation autologous chondrocyte implantation versus microfracture. The American Journal of Sports Medicine, 39, 2549–2557. doi:10.1177/0363546511420688

Kreuz, P. C., Steinwachs, M. R., Erggelet, C., Krause, S. J., Konrad, G., Uhl, M., & Südkamp, N. (2006). Results after microfracture of full-thickness chondral defects in different compartments in the knee. Osteoarthritis and Cartilage, 14, 1119-1125. doi:10.1016/j.joca.2006.05.003

Krishnan, Y., & Grodzinsky, A. J. (2018). Cartilage diseases. Matrix Biology, 71-72, 51-69. doi:10.1016/j.matbio.2018.05.005

Kusano, T., Jakob, R. P., Gautier, E., Magnussen, R. A., Hoogewoud, H., & Jacobi, M. (2012). Treatment of isolated chondral and osteochondral defects in the knee by autologous matrix-induced chondrogenesis (AMIC). Knee Surgery, Sports Traumatology, Arthroscopy, 20, 2109–2115. doi:10.1007/s00167-011-1840-2

Kwon, H., Paschos, N. K., Hu, J. C., & Athanasiou, K. (2016). Articular cartilage tissue engineering: the role of signaling molecules. Cellular and Molecular Life Sciences, 73, 1173-1194. doi:10.1007/s00018-015-2115-8

Lane, R. S., Fu, Y., Matsuzaki, S., Kinter, M., Humphries, K. M., & Griffin, T. M. (2015). Mitochondrial respiration and redox coupling in articular chondrocytes. Arthritis Research & Therapy, 17, 54. doi:10.1186/s13075-015-0566-9

Lawrence, R. C., Felson, D. T., Helmick, C. G., Arnold, L. M., Choi, H., Deyo, R. A., Gabriel, S., Hirsch, R., Hochberg, M. C., Hunder, G. G., Jordan, J. M., Katz, J. N., Kremers, H. M., & Wolfe, F. (2008). Estimates of the prevalence of arthritis and other rheumatic conditions in the United States. Part II. Arthritis & Rheumatism, 58, 26-35. doi:10.1002/art.23176

Lei, M., Liu, S. Q., & Liu, Y. L. (2008). Resveratrol protects bone marrow mesenchymal stem cell derived chondrocytes cultured on chitosan-gelatin

scaffolds from the inhibitory effect of interleukin-1beta. Acta Pharmacologica Sinica, 29, 1350-1356. doi:10.1111/j.1745-7254.2008.00880.x

Leung, G. J., Rainsford, K. D., & Kean, W. F. (2014). Osteoarthritis of the hand I: aetiology and pathogenesis, risk factors, investigation and diagnosis. Journal of Pharmacy and Pharmacology, 66, 339-346. doi:10.1111/jphp.12196

Li, W., Cai, L., Zhang, Y., Cui, L., & Shen, G. (2015). Intra-articular resveratrol injection prevents osteoarthritis progression in a mouse model by activating SIRT1 and thereby silencing HIF-2α. Journal of Orthopaedic Research, 33, 1061-1070. doi:10.1002/jor.22859

Lin, T. H., Wang, H. C., Cheng, W. H., Hsu, H. C., & Yeh, M. L. (2019). Osteochondral tissue regeneration using a tyramine-modified bilayered PLGA scaffold combined with articular chondrocytes in a porcine model. International Journal of Molecular Sciences, 20, E326. doi:10.3390/ijms20020326

Linn, F. C., & Sokoloff, L. (1965). Movement and composition of interstitial fluid of cartilage. Arthritis & Rheumatism, 8, 481-494. doi:10.1002/art.1780080402

Little, C. B., Barai, A., Burkhardt, D., Smith, S. M., Fosang, A. J., Werb, Z., Shah, M., & Thompson, E. W. (2009) Matrix metalloproteinase 13-deficient mice are resistant to osteoarthritic cartilage erosion but not chondrocyte hypertrophy or osteophyte development. Arthritis & Rheumatism, 60, 3723-3733. doi:10.1002/art.25002

Litwic, A., Edwards, M. H., Dennison, E. M., & Cooper, C. (2013). Epidemiology and burden of osteoarthritis. British Medical Bulletin, 105, 185–199. doi:10.1093/bmb/lds038

Liu, F. C., Hung, L. F., Wu, W. L., Chang, D. M., Huang, C. Y., Lai, J. H., & Ho, L. J. (2010). Chondroprotective effects and mechanisms of resveratrol in advanced glycation end products-stimulated chondrocytes. Arthritis Research & Therapy, 12, R167. doi:10.1186/ar3127

Loeser, R. F., Collins, J. A., & Diekman, B. O. (2016). Ageing and the pathogenesis of osteoarthritis. Nature Reviews Rheumatology, 12, 412–420. doi:10.1038/nrrheum.2016.65

Loeser, R. F., Gandhi, U., Long, D. L., Yin, W., & Chubinskaya, S. (2014). Aging and oxidative stress reduce the response of human articular chondrocytes

to insulin-like growth factor 1 and osteogenic protein 1. Arthritis & Rheumatology, 66, 2201–2209. doi:10.1002/art.38641

Loeser, R. F., Goldring, S. R., Scanzello, C. R., & Goldring, M. B. (2012). Osteoarthritis: a disease of the joint as an organ. Arthritis & Rheumatism, 64, 1697-1707. doi:10.1002/art.34453

Lopes, E. B. P., Filiberti, A., Husain, S. A., & Humphrey, M. B. (2017). Immune contributions to osteoarthritis. Current Osteoporosis Reports, 15, 593-600. doi:10.1007/s11914-017-0411-y

Lotz, M., & Loeser, R. F. (2012). Effects of aging on articular cartilage homeostasis. Bone, 51, 241–248. doi:10.1016/j.bone.2012.03.023

Maepa, M., Razwinani, M., & Motaung, S. (2016). Effects of resveratrol on collagen type II protein in the superficial and middle zone chondrocytes of porcine articular cartilage. Journal of Ethnopharmacology, 178, 25-33. doi:10.1016/j.jep.2015.11.047

Makris, E. A., Gomoll, A. H., Malizos, K. N., Hu, J. C., & Athanasiou, K. A. (2015). Repair and tissue engineering techniques for articular cartilage. Nature Reviews Rheumatology, 11, 21-34. doi:10.1038/nrrheum.2014.157

Makris, E. A., MacBarb, R. F., Responte, D. J., Hu, J. C., & Athanasiou, K. A. (2013). A copper sulfate and hydroxylysine treatment regimen for enhancing collagen cross-linking and biomechanical properties in engineered neocartilage. The FASEB Journal, 27, 2421–2430. doi:10.1096/fj.12-224030

Malda, J., Benders, K. E., Klein, T. J., De Grauw, J. C., Kik, M. J., Hutmacher, D. W., Saris, D. B., van Weeren, P. R., & Dhert, W. J. (2012). Comparative study of depth-dependent characteristics of equine and human osteochondral tissue from the medial and lateral femoral condyles. Osteoarthritis and Cartilage, 20, 1147-1151. doi:10.1016/j.joca.2012.06.005

Maneiro, E., Martín, M. A., de Andres, M. C., López-Armada, M. J., Fernández-Sueiro, J. L., del Hoyo, P., Galdo, F., Arenas, J., & Blanco, F. J. (2003). Mitochondrial respiratory activity is altered in osteoarthritic human articular chondrocytes. Arthritis & Rheumatism, 48, 700–708. doi:10.1002/art.10837

Marcacci, M., Berruto, M., Brocchetta, D., Delcogliano, A., Ghinelli, D., Gobbi, A., Kon, E., Pederzini, L., Rosa, D., Sacchetti, G. L., Stefani, G., & Zanasi,

S. (2005). Articular cartilage engineering with Hyalograft C: 3-year clinical results. Clinical Orthopaedics and Related Research, 435, 96–105.

Marlovits, S., Aldrian, S., Wondrasch, B., Zak, L., Albrecht, C., Welsch, G., & Trattnig, S. (2012). Clinical and radiological outcomes 5 years after matrix-induced autologous chondrocyte implantation in patients with symptomatic, traumatic chondral defects. The American Journal of Sports Medicine, 40, 2273-2280. doi:10.1177/0363546512457008

Maroudas, A., Wachtel, E., Grushko, G., Katz, E. P., & Weinberg, P. (1991). The effect of osmotic and mechanical pressures on water partitioning in articular cartilage. Biochimica et Biophysica Acta - General Subjects, 1073, 285–294.

Martel-Pelletier, J., Pelletier, J. P., & Fahmi, H. (2003). Cyclooxygenase-2 and prostaglandins in articular tissues. Seminars in Arthritis and Rheumatism, 33, 155-167. doi:10.1016/s0049-0172(03)00134-3

Mitsuyama, H., Healey, R. M., Terkeltaub, R. A., Coutts, R. D., & Amiel, D. (2007). Calcification of human articular knee cartilage is primarily an effect of aging rather than osteoarthritis. Osteoarthritis and Cartilage, 15, 559–565. doi:10.1016/j.joca.2006.10.017

Mobasheri, A. (2013). The future of osteoarthritis therapeutics: emerging biological therapy. Current Rheumatology Reports, 15, 385. doi:10.1007/s11926-013-0385-4

Mobasheri, A., Rayman, M. P., Gualillo, O., Sellam, J., van der Kraan, P., & Fearon, U. (2017). The role of metabolism in the pathogenesis of osteoarthritis. Nature Reviews Rheumatology, 13, 302–311. doi:10.1038/nrrheum.2017.50

Mow, V. C., & Guo, X. E. (2002). Mechano-electrochemical properties of articular cartilage: their inhomogeneities and anisotropies. Annual Review of Biomedical Engineering, 4, 175–209. doi:10.1146/annurev.bioeng.4.110701.120309

Mouw, J. K., Ou, G., & Weaver, V. M. (2014). Extracellular matrix assembly: a multiscale deconstruction. Nature Reviews Molecular Cell Biology, 15, 771-785. doi:10.1038/nrm3902

Muthuri, S. G., McWilliams, D. F., Doherty, M., & Zhang, W. (2011). History of knee injuries and knee osteoarthritis: a meta-analysis of observational studies. Osteoarthritis and Cartilage, 19, 1286–1293. doi:10.1016/j.joca.2011.07.015

Nguyen, C., Boutron, I., Baron, G., Coudeyre, E., Berenbaum, F., Poiraudeau, S., & Rannou, F. (2017). Evolution of pain at 3 months by oral resveratrol in knee osteoarthritis (ARTHROL): protocol for a multicentre randomised double-blind placebo-controlled trial. BMJ Open, 7, e017652. doi:10.1136/bmjopen-2017-017652

Øiestad, B. E., Engebretsen, L., Storheim, K., & Risberg, M. A. (2009). Knee osteoarthritis after anterior cruciate ligament injury. The American Journal of Sports Medicine, 37, 1434–1443. doi:10.1177/0363546509338827

Palazzo, C., Nguyen, C., Lefevre-Colau, M.-M., Rannou, F., & Poiraudeau, S. (2016). Risk factors and burden of osteoarthritis. Annals of Physical and Rehabilitation Medicine, 59, 134–138. doi:10.1016/j.rehab.2016.01.006

Pan, J., Zhou, X., Li, W., Novotny, J. E., Doty, S. B., & Wang, L. (2009). In situ measurement of transport between subchondral bone and articular cartilage. Journal of Orthopaedic Research, 27, 1347–1352. doi:10.1002/jor.20883

Pelletier, J. P., Martel-Pelletier, J., & Abramson, S. B. (2001). Osteoarthritis, an inflammatory disease: potential implication for the selection of new therapeutic targets. Arthritis & Rheumatism, 44, 1237-1247. doi:10.1002/1529-0131(200106)44:6<1237::AID-ART214>3.0.CO;2-F

Peterson, L., Minas, T., Brittberg, M., Nilsson, A., Sjögren-Jansson, E., & Lindahl, A. (2000). Two- to 9-year outcome after autologous chondrocyte transplantation of the knee. Clinical Orthopaedics and Related Research, 374, 212–234. doi:10.1097/00003086-200005000-00020

Peterson, L., Vasiliadis, H. S., Brittberg, M., & Lindahl, A. (2010). Autologous chondrocyte implantation: a long-term follow-up. The American Journal of Sports Medicine, 38, 1117–1124. doi:10.1177/0363546509357915

Petersson, I. F., Boegård, T., Saxne, T., Silman, A. J., & Svensson, B. (1997). Radiographic osteoarthritis of the knee classified by the Ahlbäck and Kellgren & Lawrence systems for the tibiofemoral joint in people aged 35-54 years with chronic knee pain. Annals of the Rheumatic Diseases, 56, 493–496. doi:10.1136/ard.56.8.493

Pietkiewicz, J., Danielewicz, R., Bednarz-Misa, I. S., Ceremuga, I., Wiśniewski, J., Mierzchala-Pasierb, M., Bronowicka-Szydełko, A., Ziomek, E., & Gamian, A. (2018). Experimental and bioinformatic approach to identifying antigenic epitopes in human α- and β-enolases. Biochemistry and Biophysics Reports, 15, 25-32. doi:10.1016/j.bbrep.2018.05.008

Poole, C. A. (1997). Articular cartilage chondrons: form, function and failure. Journal of Anatomy, 191, 1-13. doi:10.1046/j.1469-7580.1997.19110001.x

Poole, C. A., Flint, M. H., & Beaumont, B. W. (1984). Morphological and functional interrelationships of articular cartilage matrices. Journal of Anatomy, 138, 113–138.

Qin, N., Wei, L., Li, W., Yang, W., Cai, L., Qian, Z., & Wu, S. (2017). Local intra-articular injection of resveratrol delays cartilage degeneration in C57BL/6 mice by inducing autophagy via AMPK/mTOR pathway. Journal of Pharmacological Sciences, 134, 166–174. doi:10.1016/j.jphs.2017.06.002

Rengel, Y., Ospelt, C., & Gay, S. (2007). Proteinases in the joint: clinical relevance of proteinases in joint destruction. Arthritis Research & Therapy, 9, 221. doi:10.1186/ar2304

Richette, P., Poitou, C., Garnero, P., Vicaut, E., Bouillot, J.-L., Lacorte, J.-M., Basdevant, A., Clément, K., Bardin, T., & Chevalier, X. (2011). Benefits of massive weight loss on symptoms, systemic inflammation and cartilage turnover in obese patients with knee osteoarthritis. Annals of the Rheumatic Diseases, 70, 139–144. doi:10.1136/ard.2010.134015

Robinson, W. H., Lepus, C. M., Wang, Q., Raghu, H., Mao, R., Lindstrom, T. M., & Sokolove, J. (2016). Low-grade inflammation as a key mediator of the pathogenesis of osteoarthritis. Nature Reviews Rheumatology, 12, 580-592. doi:10.1038/nrrheum.2016.136

Rosano, C. L., Braun, C. B., & Hurwitz, C. (1987). A method for serum C1q based on its hydroxyproline content. Clinical Chemistry, 33, 398-400.

Schmidt, T. A., Gastelum, N. S., Nguyen, Q. T., Schumacher, B. L., & Sah, R. L. (2007). Boundary lubrication of articular cartilage: role of synovial fluid constituents. Arthritis & Rheumatism, 56, 882–891. doi:10.1002/art.22446

Schulze-Tanzil, G., Mobasheri, A., Sendzik, J., John, T., & Shakibaei, M. (2004). Effects of curcumin (diferuloylmethane) on nuclear factor kappaB signaling in interleukin-1beta-stimulated chondrocytes. Annals of the New York Academy of Sciences, 1030, 578-586. doi:10.1196/annals.1329.067

Schulze-Tanzil, G., Müller, R. D., Kohl, B., Schneider, N., Ertel, W., Ipaktchi, K., Hünigen, H., Gemeinhardt, O., Stark, R., & John, T. (2009). Differing in vitro biology of equine, ovine, porcine and human articular chondrocytes

derived from the knee joint: an immunomorphological study. Histochemistry and Cell Biology, 131, 219-229. doi:10.1007/s00418-008-0516-6

Shakibaei, M., Csaki, C., Nebrich, S., & Mobasheri, A. (2008). Resveratrol suppresses interleukin-1beta-induced inflammatory signaling and apoptosis in human articular chondrocytes: potential for use as a novel nutraceutical for the treatment of osteoarthritis. Biochemical Pharmacology, 76, 1426-1439. doi:10.1016/j.bcp.2008.05.029

Shakibaei, M., John, T., Seifarth, C., & Mobasheri, A. (2007). Resveratrol inhibits IL-1 beta-induced stimulation of caspase-3 and cleavage of PARP in human articular chondrocytes in vitro. Annals of the New York Academy of Sciences, 1095, 554-563. doi:10.1196/annals.1397.060

Shakibaei, M., Mobasheri, A., & Buhrmann, C. (2011). Curcumin synergizes with resveratrol to stimulate the MAPK signaling pathway in human articular chondrocytes in vitro. Genes & Nutrition, 6, 171-179. doi:10.1007/s12263-010-0179-5

Sharma, L., Song, J., Felson, D. T., Cahue, S., Shamiyeh, E., & Dunlop, D. D. (2001). The role of knee alignment in disease progression and functional decline in knee osteoarthritis. Journal of the American Medical Association, 286, 188–195. doi:10.1001/jama.286.2.188

Shen, C. L., Smith, B. J., Lo, D. F., Chyu, M. C., Dunn, D. M., Chen, C. H., & Kwun, I. S. (2012). Dietary polyphenols and mechanisms of osteoarthritis. The Journal of Nutritional Biochemistry, 23, 1367-1377. doi:10.1016/j.jnutbio.2012.04.001

Sheu, S. Y., Chen, W. S., Sun, J. S., Lin, F. H., & Wu, T. (2013). Biological characterization of oxidized hyaluronic acid/resveratrol hydrogel for cartilage tissue engineering. Journal of Biomedical Materials Research Part A, 101, 3457-3466. doi:10.1002/jbm.a.34653

Siclari, A., Mascaro, G., Gentili, C., Cancedda, R., & Boux, E. (2012). A cell-free scaffold-based cartilage repair provides improved function hyaline-like repair at one year. Clinical Orthopaedics and Related Research, 470, 910–919. doi:10.1007/s11999-011-2107-4

Slauterbeck, J. R., Kousa, P., Clifton, B. C., Naud, S., Tourville, T. W., Johnson, R. J., & Beynnon, B. D. (2009). Geographic mapping of meniscus and cartilage lesions associated with anterior cruciate ligament injuries. The Journal of Bone & Joint Surgery, 91, 2094–2103. doi:10.2106/JBJS.H.00888

Sohn, D. H., Sokolove, J., Sharpe, O., Erhart, J. C., Chandra, P. E., Lahey, L. J., Lindstrom, T. M., Hwang, I., Boyer, K. A., Andriacchi, T. P., & Robinson, W. H. (2012). Plasma proteins present in osteoarthritic synovial fluid can stimulate cytokine production via Toll-like receptor 4. Arthritis Research & Therapy, 14, R7. doi:10.1186/ar3555

Sokolove, J., & Lepus, C. M. (2013). Role of inflammation in the pathogenesis of osteoarthritis: latest findings and interpretations. Therapeutic Advances in Musculoskeletal Disease, 5, 77-94. doi:10.1177/1759720X12467868

Spector, T. D., & MacGregor, A. J. (2004). Risk factors for osteoarthritis: genetics. Osteoarthritis and Cartilage, 12, S39-S44. doi:10.1016/j.joca.2003.09.005

Srikanth, V. K., Fryer, J. L., Zhai, G., Winzenberg, T. M., Hosmer, D., & Jones, G. (2005). A meta-analysis of sex differences prevalence, incidence and severity of osteoarthritis. Osteoarthritis and Cartilage, 13, 769–781. doi:10.1016/j.joca.2005.04.014

Steinwachs, M. R., Gille, J., Volz, M., Anders, S., Jakob, R., de Girolamo, L., Volpi, P., Schiavone-Panni, A., Scheffler, S., Reiss, E., & Wittmann, U. (2019). Systematic review and meta-analysis of the clinical evidence on the use of autologous matrix-induced chondrogenesis in the knee. Cartilage. doi:10.1177/1947603519870846

Stichler, S., Böck, T., Paxton, N., Bertlein, S., Levato, R., Schill, V., Smolan, W., Malda, J., Teßmar, J., Blunk, T., & Groll, J. (2017). Double printing of hyaluronic acid/poly(glycidol) hybrid hydrogels with poly(epsilon-caprolactone) for MSC chondrogenesis. Biofabrication, 9, 044108. doi:10.1088/1758-5090/aa8cb7

Thoms, B. L., Dudek, K. A., Lafont, J. E., & Murphy, C. L. (2013). Hypoxia promotes the production and inhibits the destruction of human articular cartilage. Arthritis & Rheumatism, 65, 1302-1312. doi:10.1002/art.37867

Tonge, D. P., Pearson, M. J., & Jones, S. W. (2014). The hallmarks of osteoarthritis and the potential to develop personalised disease-modifying pharmacological therapeutics. Osteoarthritis and Cartilage, 22, 609-621. doi:10.1016/j.joca.2014.03.004

Ulrich-Vinther, M., Maloney, M. D., Schwarz, E. M., Rosier, R., & O'Keefe, R. J. (2003). Articular cartilage biology. Journal of the American Academy of Orthopaedic Surgeons, 11, 421–430. doi:10.5435/00124635-200311000-00006

Vaamonde-García, C., Riveiro-Naveira, R. R., Valcárcel-Ares, M. N., Hermida-Carballo, L., Blanco, F. J., & López-Armada, M. J. (2012). Mitochondrial dysfunction increases inflammatory responsiveness to cytokines in normal human chondrocytes. Arthritis & Rheumatism, 64, 2927–2936. doi:10.1002/art.34508

Verbruggen, G., Wittoek, R., Vander Cruyssen, B., & Elewaut, D. (2012). Tumour necrosis factor blockade for the treatment of erosive osteoarthritis of the interphalangeal finger joints: a double blind, randomised trial on structure modification. Annals of the Rheumatic Diseases, 71, 891-898. doi:10.1136/ard.2011.149849

Vinardell, T., Sheehy, E. J., Buckley, C. T., & Kelly, D. J. (2012). A comparison of the functionality and in vivo phenotypic stability of cartilaginous tissues engineered from different stem cell sources. Tissue Engineering Part A, 18, 1161-1170. doi:10.1089/ten.tea.2011.0544

Vos, T., Flaxman, A. D., Naghavi, M., Lozano, R., Michaud, C., Ezzati, M., Shibuya, K., Salomon, J. A., Abdalla, S., Aboyans, V., Abraham, J., Ackerman, I., Aggarwal, R., Ahn, S. Y., Ali, M. K., AlMazroa, M. A., Alvarado, M., Anderson, H. R., Anderson, L. M., . . . Murray, C. J. L. (2012). Years lived with disability (YLDs) for 1160 sequelae of 289 diseases and injuries 1990–2010: a systematic analysis for the Global Burden of Disease Study 2010. The Lancet, 380, 2163–2196. doi:10.1016/S0140-6736(12)61729-2

Wallace, I. J., Worthington, S., Felson, D. T., Jurmain, R. D., Wren, K. T., Maijanen, H., Woods, R. J., & Lieberman, D. E. (2017). Knee osteoarthritis has doubled in prevalence since the mid-20th century. Proceedings of the National Academy of Sciences of the United States of America, 114, 9332-9336. doi:10.1073/pnas.1703856114

Walle, T (2011). Bioavailability of resveratrol. Annals of the New York Academy of Sciences, 1215, 9-15. doi:10.1111/j.1749-6632.2010.05842.x

Wang, J., Gao, J. S., Chen, J. W., Li, F., & Tian, J. (2012). Effect of resveratrol on cartilage protection and apoptosis inhibition in experimental osteoarthritis of rabbit. Rheumatology International, 32, 1541-1548. doi: 10.1007/s00296-010-1720-y

Wang, Y., Zhao, X., Lotz, M., Terkeltaub, R., & Liu-Bryan, R. (2015). Mitochondrial biogenesis is impaired in osteoarthritis chondrocytes but reversible via peroxisome proliferator-activated receptor γ coactivator 1α. Arthritis & Rheumatology, 67, 2141–2153. doi:10.1002/art.39182

Watt, F. M. (1988). Effect of seeding density on stability of the differentiated phenotype of pig articular chondrocytes in culture. Journal of Cell Science, 89, 373-378.

Woessner, J. F. J. (1961). The determination of hydroxyproline in tissue and protein samples containing small proportions of this imino acid. Archives of Biochemistry and Biophysics, 93, 440-447. doi:10.1016/0003-9861(61)90291-0

Xia, B., Chen, D., Zhang, J., Hu, S., Jin, H., & Tong, P. (2014). Osteoarthritis pathogenesis: a review of molecular mechanisms. Calcified Tissue International, 95, 495-505. doi:10.1007/s00223-014-9917-9

Yin, L., Wu, Y., Yang, Z., Denslin, V., Ren, X., Tee, C. A., Lai, Z., Lim, C. T., Han, J., & Lee, E. H. (2018). Characterization and application of size-sorted zonal chondrocytes for articular cartilage regeneration. Biomaterials, 165, 66-78. doi:10.1016/j.biomaterials.2018.02.050

Yin, W., Park, J.-I., & Loeser, R. F. (2009). Oxidative stress inhibits insulin-like growth factor-I induction of chondrocyte proteoglycan synthesis through differential regulation of phosphatidylinositol 3-Kinase-Akt and MEK-ERK MAPK signaling pathways. The Journal of Biological Chemistry, 284, 31972–31981. doi:10.1074/jbc.M109.056838

Yu, F., Li, M., Yuan, Z., Rao, F., Fang, X., Jiang, B., Wen, Y., & Zhang, P. (2018). Mechanism research on a bioactive resveratrol-PLA-gelatin porous nano-scaffold in promoting the repair of cartilage defect. International Journal of Nanomedicine, 13, 7845-7858. doi:10.2147/IJN.S181855

Part VII

Appendix

Abbreviations

3D	three-dimensional
ACI	autologous chondrocyte implantation
ACL	anterior cruciate ligament
Actb	beta-actin
AGE	advanced glycation end-product
AMIC	autologous matrix-induced chondrogenesis
ANOVA	analysis of variance
AP-1	activator protein 1
ATP	adenosine triphosphate
BMI	body mass index
BMP	bone morphogenetic protein
BSA	bovine serum albumin
cDNA	complementary deoxyribonucleic acid
COL I	collagen type I
COL II	collagen type II
COL X	collagen type X
COX-2	cyclooxygenase-2
DAB	dimethylaminobenzaldehyde
DAMP	damage-associated molecular pattern
DAPI	4',6-diamidino-2-phenylindole
ddH2O	double-distilled water
DMEM	Dulbecco's Modified Eagle's Medium
DMMB	dimethylmethylene blue
DNA	deoxyribonucleic acid

ECM	extracellular matrix
EDTA	ethylenediaminetetraacetic acid
ESR	erythrocyte sedimentation rate
FBS	fetal bovine serum
GAG	glycosaminoglycan
HEPES	4-(2-hydroxyethyl)-1-piperazineethanesulfonic acid
IGF-1	insulin-like growth factor 1
IgG	immunoglobulin G
IHC	immunohistochemistry
IL-1β	interleukin 1β
ITS+	insulin-transferrin-selenium-plus
LPS	lipopolysaccharide
MACI	matrix-induced autologous chondrocyte implantation
MAPK	mitogen-activated protein kinase
MMP	matrix metalloproteinase
mRNA	messenger ribonucleic acid
MSC	mesenchymal stem cell
NEAA	non-essential amino acids
NF-κB	nuclear factor κB
NSAID	non-steroidal anti-inflammatory drug
OA	osteoarthritis
P1	first passage cells
PARP	poly(ADP-ribose)polymerase
PBE	polybuffer exchanger
PBS	phosphate-buffered saline
PGE2	prostaglandin E2
PLA	polylactide

qRT-PCR	quantitative real-time polymerase chain reaction
RA	rheumatoid arthritis
RNA	ribonucleic acid
ROS	reactive oxygen species
RSV	resveratrol
SD	standard deviation
SF	synovial fluid
TBS	tris-buffered saline
TBST	tris-buffered saline with Tween 20
TGF-1β	transforming growth factor β1
TNFα	tumor necrosis factor α
VEGF	vascular endothelial growth factor

List of Figures

List of Tables

Acknowledgments

An erster Stelle möchte ich mich ganz besonders bei Herrn Prof. Dr. Torsten Blunk für die Vergabe dieses Promotionsprojektes und die Aufnahme in seine Arbeitsgruppe bedanken. Bei fachlichem Austausch vermittelte er zahlreiche anregende Aspekte und hat damit meine Begeisterung für wissenschaftliches Arbeiten grundlegend geprägt. Für die intensive persönliche Betreuung bei der Publikation dieses Projektes bedanke ich mich herzlich.

Herrn Prof. Dr. Rainer Meffert danke ich außerordentlich für die freundliche Unterstützung und überaus interessanten Gespräche unter anderem beim Deutschen Kongress für Orthopädie und Unfallchirurgie 2018.

Oliver Berberich gilt mein ausdrücklicher Dank für seine intensive und engagierte Betreuung im Labor. Besonders seine bemerkenswerte Geduld und sein unverwechselbarer Humor waren sehr wertvoll.

Ein großes Dankeschön geht zudem an Thomas Böck für die ausgezeichnete Zusammenarbeit bei methodischen Herausforderungen.

Sabine Müller-Morath möchte ich besonders für die intensive und flexible Mitwirkung im Labor danken.

Der gesamten Arbeitsgruppe danke ich für die hervorragende Stimmung und den Zusammenhalt während dieser gemeinsamen Zeit im Labor.

Mein ganz besonderer Dank gilt Kathrin für ihre Ratschläge und Korrekturen während der Erstellung dieser Arbeit.

Schließlich möchte ich Rita und Richard außerordentlich für die Ermöglichung einer universitären Ausbildung sowie die fortwährende Unterstützung im Rahmen dieser Doktorarbeit danken.

Publications and Conference Contributions

Journal Articles

Frischholz, S., Berberich, O., Böck, T., Meffert, R., & Blunk, T. (2020). Resveratrol counteracts IL-1β-mediated impairment of extracellular matrix deposition in 3D articular chondrocyte constructs. Journal of Tissue Engineering and Regenerative Medicine, 14, 897-908. doi: 10.1002/term.3031

Oral Presentations

Frischholz, S., Berberich, O., Böck, T., Meffert, R., & Blunk, T. (2018). Resveratrol counteracts IL-1 beta induced degradation of 3D articular chondrocyte constructs in vitro. German Congress of Orthopaedics and Traumatology (DKOU) 2018, Berlin, Germany.

Statement on Copyright and Self-plagiarism

The data presented in this thesis have been partially published in the *Journal of Tissue Engineering and Regenerative Medicine* as an original article entitled "Resveratrol counteracts IL-1β-mediated impairment of extracellular matrix deposition in 3D articular chondrocyte constructs". In accordance with the regulations of the parent publisher Wiley (License CC BY-NC 4.0), data, text passages and illustrations from the final published manuscript were used in identical or modified form in this thesis. The Figures 3.1, 4.2, 4.3, 4.5, and 4.6 within this thesis have been previously published in a modified or identical design in the original article:

Frischholz, S., Berberich, O., Böck, T., Meffert, R., & Blunk, T. (2020). Resveratrol counteracts IL-1β-mediated impairment of extracellular matrix deposition in 3D articular chondrocyte constructs. Journal of Tissue Engineering and Regenerative Medicine, 14, 897-908. doi: 10.1002/term.3031

Statement of individual contributions: I, Sebastian Frischholz, designed the study, conducted the experiments, evaluated the data and wrote the manuscript. Oliver Berberich contributed to the study design, methods refinement, and was involved in the proofreading. Thomas Böck supported the methods refinement and data collection. Rainer Meffert was involved in the study design and proofreading. Torsten Blunk, as principal investigator, participated in the study design, data interpretation, manuscript writing, and proofreading.